AD-A080 769 BENDIX CORP BALTIMORE MD COMMUNICATIONS DIV F/G 9/5
TACTICAL MINIATURE CRYSTAL OSCILLATOR,(U)
DEC 79 D L HARTON, D BROWN DAAB07-78-C-2990
UNCLASSIFIED DELET-TR-78-2990-1 NL

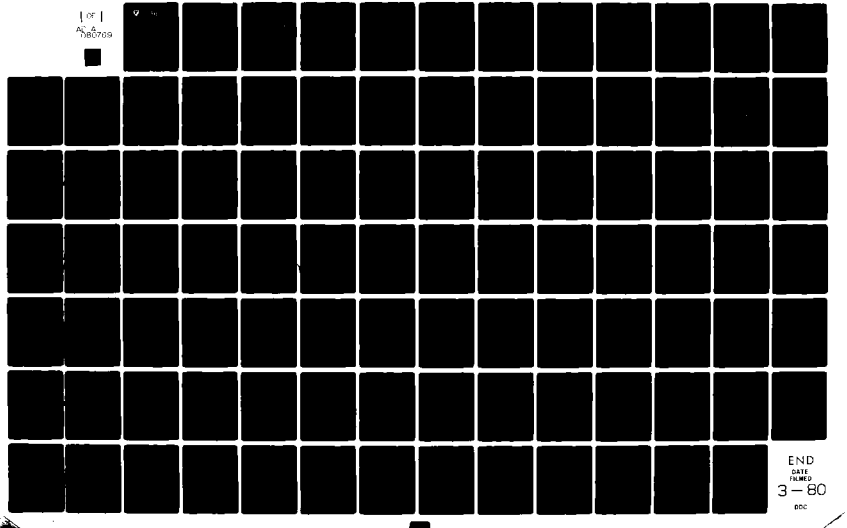

END
DATE FILMED
3-80
DDC

Research and Development Technical Report

DELET-TR-78-2990-1

TACTICAL MINIATURE CRYSTAL OSCILLATOR

D. L. Harton
D. Brown

THE BENDIX CORPORATION
COMMUNICATIONS DIVISION
East Joppa Road
Baltimore, Maryland 21204

402 895

December 1979

Semiannual Report 1 October 1978 – 1 April 1979

PREPARED FOR

ERADCOM

US ARMY ELECTRONICS RESEARCH AND DEVELOPMENT COMMAND
FORT MONMOUTH, NEW JERSEY 07703

NOTICES

Disclaimers

The findings in this report are not be be construed as an official Department of the Army position, unless so designated by other authorized documents.

The citation of trade names and names of manufacturers in this report is not to be construed as official Government indorsement or approval of commercial products or services referenced herein.

Disposition

Destroy this report when it is no longer needed. Do not return it to the originator.

The electronics assembly consisting of two hybrid substances and the crystal resonator is suspended by its leads from the header of the evacuated inner container. The inner container is in turn supported by a system of Kovar wires (which also provide electrical connections) that feed through the header of the outer container. Both the inner and outer containers are hermetically sealed and the space between the containers is evacuated. Removal of the gas between the two containers eliminates heat transfer due to gas conduction and convection. This leaves only conduction through the Kovar wires and radiation as thermal coupling mechanisms between the inner container and the outer environment.

One of the hybrid substrates making up the electronics assembly contains the thermal control and voltage regulator circuits. The second substrate contains the oscillator, AGC, and buffer amplifier circuits. Design goals, the Baseline approach, and accomplishments are described. Data on crystal/oscillator behavior and electrical mechanical design calculations are presented.

TABLE OF CONTENTS

TABLE OF CONTENTS (Cont)

LIST OF FIGURES

LIST OF FIGURES (Cont)

LIST OF TABLES

1. PURPOSE

The objective of this program is the advanced development of the Tactical Miniature Crystal Oscillator (TMXO) having capability for use as a precision frequency/time reference in advanced communications, navigation, and position location systems.

Previous work conducted under Contracts DAAB07-73-C-0199 and DAAB07-75-C-1327 with The Bendix Corporation has demonstrated the feasibility of a lightweight, low power, fast warmup precision quartz reference oscillator based upon a design which employs the vacuum of the TMXO outer enclosure as an insulating medium. In the TMXO, an integrated assembly consisting of a ceramic enclosed crystal unit bonded to a microcircuit, enclosed in a similar ceramic package, is employed to provide necessary thermal and electrical functions. A thermal support provides for both heat isolation and mechanical mounting for the crystal/microcircuit assembly. Development is to be conducted to optimize TMXO thermal, electrical, and mechanical design and fabrication processes. These procedures will be established and tests conducted to verify TMXO suitability for use over operating conditions and environments encountered in military manpack, vehicular, and airborne usage. Documentation will detail all aspects of TMXO design, process development, special tooling, and performance testing.

Specifically, the major tasks to be performed on this contract are:

Develop both 5.11 MHz and 10 MHz crystal oscillator circuits to provide an acceleration coefficient and short and long term performance consistent with meeting performance characteristics outlined below. A common hybrid microcircuit design shall be evolved permitting either 5.11 MHz (fundamental) or 10 MHz (fundamental or 3d overtone) operation with only minor modification during assembly. Precision ceramic flatpack crystal units currently in development by ERADCOM are to be employed.

Optimize TMXO electrical design using computer aided design and analysis methods to provide a high yield in circuit performance and reliability at minimum costs. The analysis is to

show that the TXMO final design will meet performance requirements under worst case element value tolerances and parameter variations.

Develop cost effective processes for fabrication of the TMXO hybrid microcircuit assembly and outer enclosure. Emphasis will be placed on obtaining reliable seals of the inner and outer enclosures which will extend the useful life of the TMXO through reduced power aging.

Design and fabricate special fixturing and tooling for assembly, bakeout, vacuum outgassing, sealing and testing of the TMXO.

Establish TMXO test procedures using Quality Conformance Procedures of MIL-O-55310 as a baseline.

Fabricate and test advanced development models of the TMXO incorporating methods and techniques evolved.

The final report is to contain a technical description of all pertinent design and development work accomplished. It will include a complete description of electrical and mechanical components, processes, procedures and fixturing which would permit reproduction of the developed oscillators.

The required characteristics of the TMXO are given below.

Case Outline. The TMXO shall approximate USAECOM outline drawing shown in Figure 1-1.

Weight. The maximum weight shall be 75 grams.

Seal. The TMXO shall be final baked and solder sealed in a vacuum of 1×10^{-5} Torr. Maximum leak rate shall be 1×10^{-12} cc/sec.

Supply Voltage. 12 V dc $\pm$5%.

Warmup Power. 10.0 watts at any ambient temperature.

Operating Power. After warmup maximum power input not to exceed 250 milliwatts at any temperature.

Power Aging. Not to exceed 1% per month.

Nominal Frequency. The nominal frequency of the TMXO shall be 5.115 MHz and 10 MHz.

Voltage Control. The output frequency deviation for a 0 to 10 V dc change applied at the voltage control terminal shall be no less than 2×10^{-7}. The voltage input impedance shall be greater than 10,000 ohms.

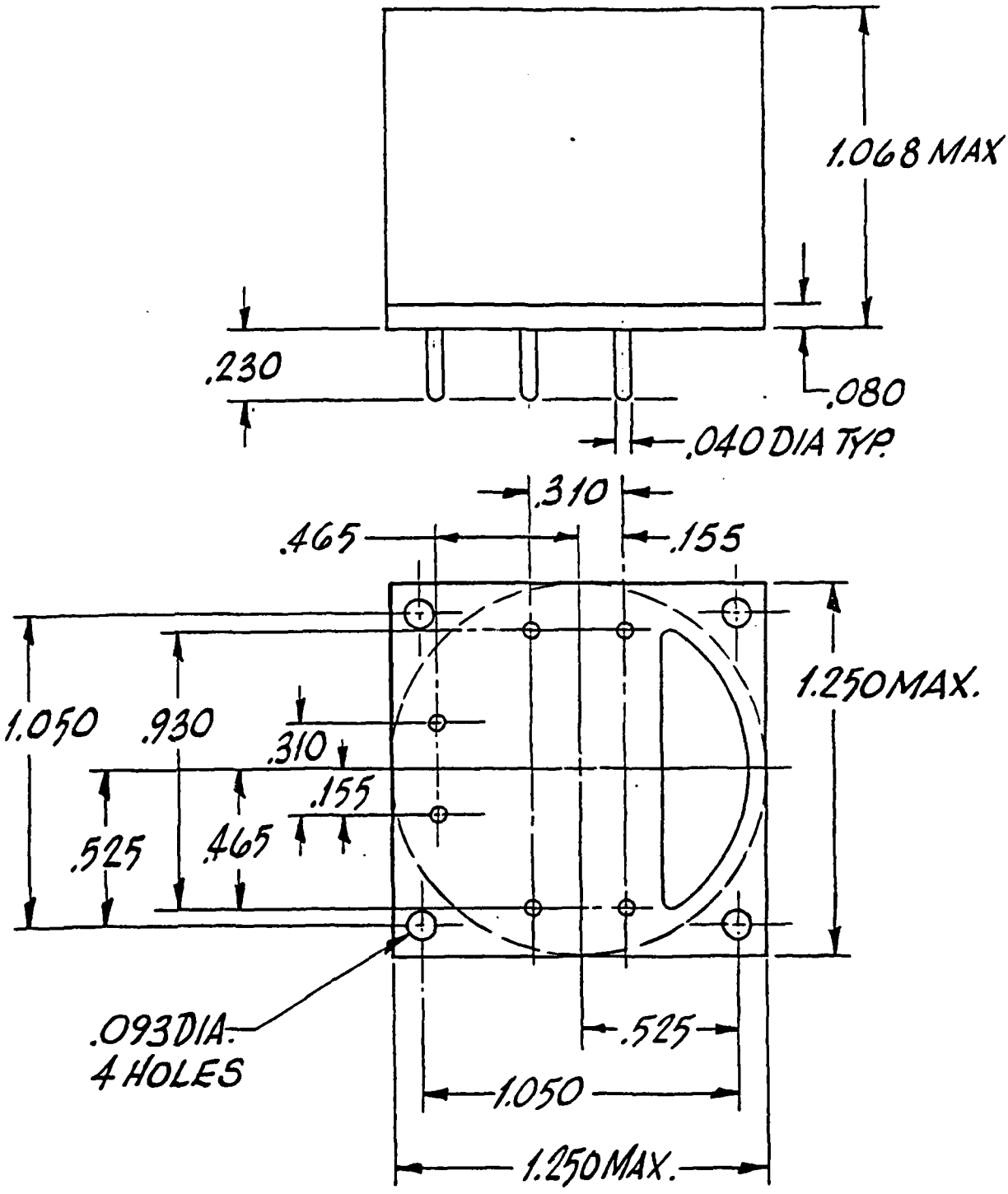

FIGURE 1-1. OUTLINE DRAWING

Frequency Adjustment. The unit shall be capable of an alternate means of frequency adjustment by termination of the voltage control terminal to ground with a multi-turn 0-100 K ohm potentiometer. The frequency setability shall be better than $\pm 1 \times 10^{-10}$ and tuning range no less than $\pm 1 \times 10^{-8}$ of nominal frequency.

Stabilization Time. Following application of power, the frequency shall be within $\pm 1 \times 10^{-8}$ of final frequency in 3 minutes.

Frequency/Temperature Stability (Steady State). The maximum permissible frequency deviation over the range of $-54^{\circ}C$ to $+75^{\circ}C$ shall be $\pm 1 \times 10^{-8}$.

Frequency/Temperature Stability (Transient). The frequency shall not change more than $\pm 1 \times 10^{-8}$ from its initial value when subjected to a positive $10^{\circ}C$ amplitude, $1^{\circ}C$/min air temperature ramp starting at $-40^{\circ}C$, $-5^{\circ}C$, $+30^{\circ}C$, and $+65^{\circ}C$.

Frequency/Acceleration Stability. The maximum frequency change measured during static acceleration shall be 1×10^{-9} when tested in accordance with Method 513, Procedure II (helicopter category) MIL-STD-810B. Permanent frequency change shall be no greater than $\pm 1 \times 10^{-9}$.

Frequency/Vibration Stability. The maximum permissible average frequency change measured during and following vibration without isolators shall be $\pm 1.0 \times 10^{-9}$ when tested in accordance with Method 514, Curve M, MIL-STD-810B. The frequency deviation represented by the modulation side bands at the vibration frequency shall not exceed 1×10^{-9} times the peak acceleration level specified for that frequency by curve M.

Frequency/Shock Stability. The maximum permissible frequency change following a shock of 50g. 11 msec shall be $\pm 1 \times 10^{-9}$ when tested in accordance with Method 213, Condition G, MIL-STD-202D.

Frequency/Attitude Stability. The maximum frequency change for a 90 $\pm 5^{\circ}$ attitude change in any axis shall be 1×10^{-9}.

Frequency/Altitude Stability. The maximum frequency change following an altitude change from sea level to 10,000 ft shall be $\pm 1 \times 10^{-9}$.

Frequency/Load Stability. The maximum frequency deviation for a load variation of 1000 ohm ±10%, 20° phase shall be ±1 x 10^{-9}.

Frequency Voltage Stability. The maximum permissible frequency deviation for a supply voltage variation of 12 volts ±5% shall be ±1 x 10^{-9}.

Frequency Aging. Aging of the output frequency shall not exceed 2 x 10^{-10} per week, operating, after a 30 day stabilization period.

Short Term Stability. The maximum rms frequency deviation shall be ±1 x 10^{-11} for averaging times ranging from 1 sec to 20 minutes under conditions of input voltage and ambient temperature controlled to ±1 mV and ±0.1°C respectively.

Frequency Recovery at -40°C Ambient. The output frequency after warmup during each turn-on period for a 5 cycle frequency recovery shall remain within ±3 x 10^{-9} of the frequency measured on the first cycle. Each cycle shall consist of complete frequency stabilization during turn-on, followed by complete thermal stabilization after power is removed.

Output Voltage. A minimum of 0.170 rms at the output frequency shall be available across an external resistive load of 1 K ohms. The output waveform shall be a sine wave.

Ambient Temperature Range. The TMXO shall meet all requirements of this specification over the ambient temperature range of -54° to +75°C.

Microcircuit Design and Construction. Microcircuit design and construction shall be in accordance with para 3.5 of MIL-M-38510. Exception for use of expoxies for non-electrical connection shall be requested in writing to the contracting office stating type, company experience and inspection and in process controls to be employed.

Quartz Crystal. Ceramic flatpack, microcircuit compatible quartz crystal units in accordance with MIL-C-3098.

Screening. The TMXO microcircuit sub-assembly shall be capable of meeting screening requirements of Method 5008, MIL-STD-883 with the following exceptions:

a. Bond Strength (para. 3.2.2.1) shall be performed on all units.

b. Temperature Cycling (para. 3.2.3.4) shall be performed in accordance with test condition B.

c. Mechanical Shock or Constant Acceleration (para. 3.2.3.5). Constant acceleration only shall be performed.

d. Omit test procedure 3.2.1.1, 3.2.3.11, 3.2.3.12, and 3.2.3.13.

Metric Dimensioning. Metric dimensioning shall be employed.

Nuclear Survivability. Consideration shall be given to the selection and development of parts, materials, processes, design details, and operating principles to insure realization of the inherent level of nuclear and EMP hardness of which the circuit/sub-system is capable. Typical radiation levels of interest fall in the ranges: 10^2 - 10^5 roentgen (cobalt 60) and 10^{12} 10^{14} neutrons/cm^2 (1 MeV equivalent). Test and/or analysis of the design shall be made to indicate the most probable modes of degradation or malfunction and to provide a first order estimate of the degrees of nuclear hardness achieved.

2. BASELINE APPROACH

The baseline approach taken is that of results obtained under Contracts DAAB07-73-C-0199 and DAAB07- 75-C-1327 and consists of the following circuits and mechanical configuration.

2A CIRCUITS.

(1) GENERAL. The electronic functions required in the implementation of the TMXO are a temperature control circuit, voltage regulator, oscillator, and buffer amplifier. The voltage regulator and temperature control circuits operate independently of other circuit functions and therefore their characteristics are more easily defined.

Of the TMXO circuits the oscillator circuit is the most complex. It consists of a passive resonant circuit composed of a quartz resonator and associated external reactances, and an active circuit which provides a precisely controlled excitation to the passive circuit.

Two oscillator circuit configurations which have been used previously for the TMXO application are described below.

(2) OSCILLATOR CIRCUIT. A modified Colpitts oscillator circuit has been used in previous TMXO designs and in many other oscillator designs. This circuit has had the benefit of extensive analysis and ample data documenting its performance is available. It therefore represents a tried and proven approach.

The circuit diagram of the Colpitts circuit used in the current version of the TMXO is shown in Figure 2-1.

The Colpitts circuit in itself, however, does not have a satisfactory mechanism for amplitude control. In precision oscillator applications, it is normally used in combination with an amplifier and detector to provide an AGC function. This circuitry is illustrated in Figure 2-2.

Although AGC has not been used in previous versions of the TMXO, it is felt that some method of crystal current control will be necessary if long term stability requirements are to be met.

(a) SELF LIMITING. An alternative to the use of AGC is to use a circuit which will limit at a level which produces the desired drive current. A circuit diagram is shown in Figure 2-3.

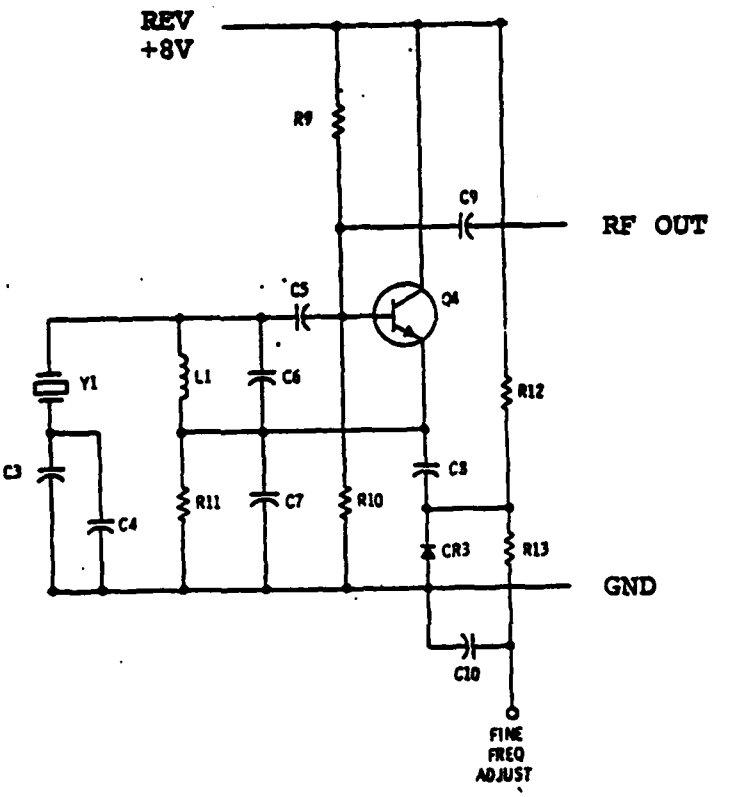

FIGURE 2-1 ~ COLPITTS OSCILLATOR CIRCUIT

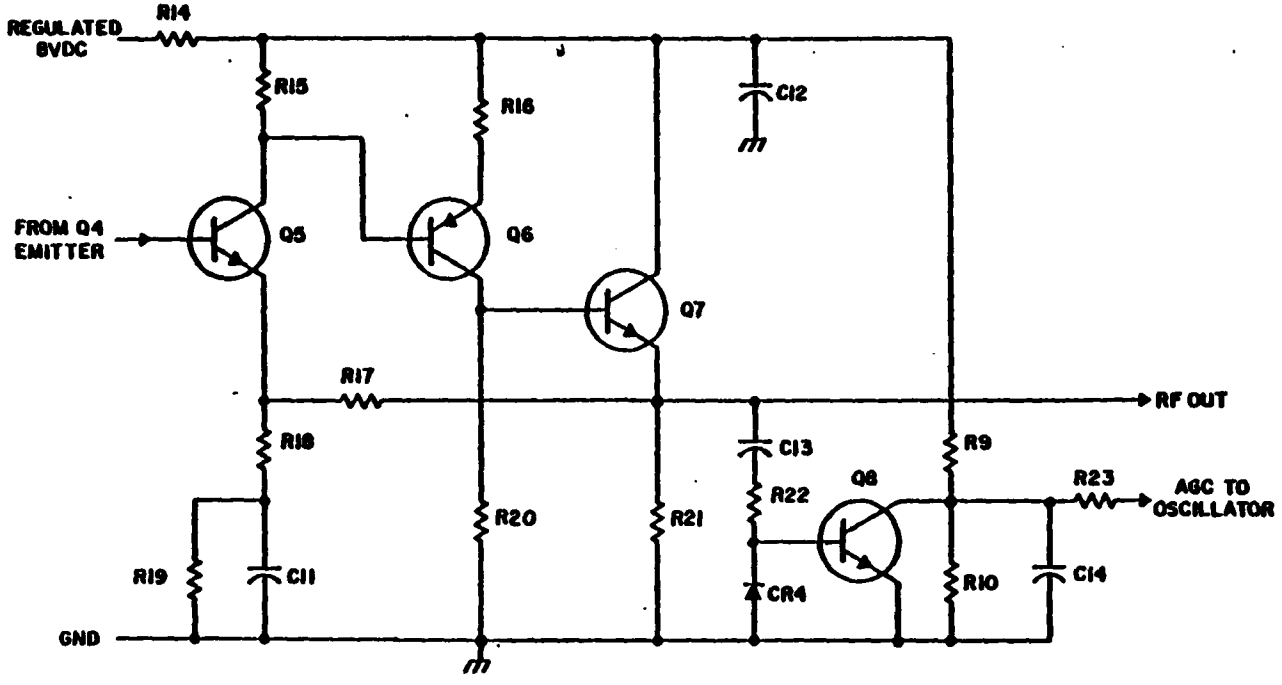

FIGURE 2-2 - AGC AMPLIFIER & DETECTOR

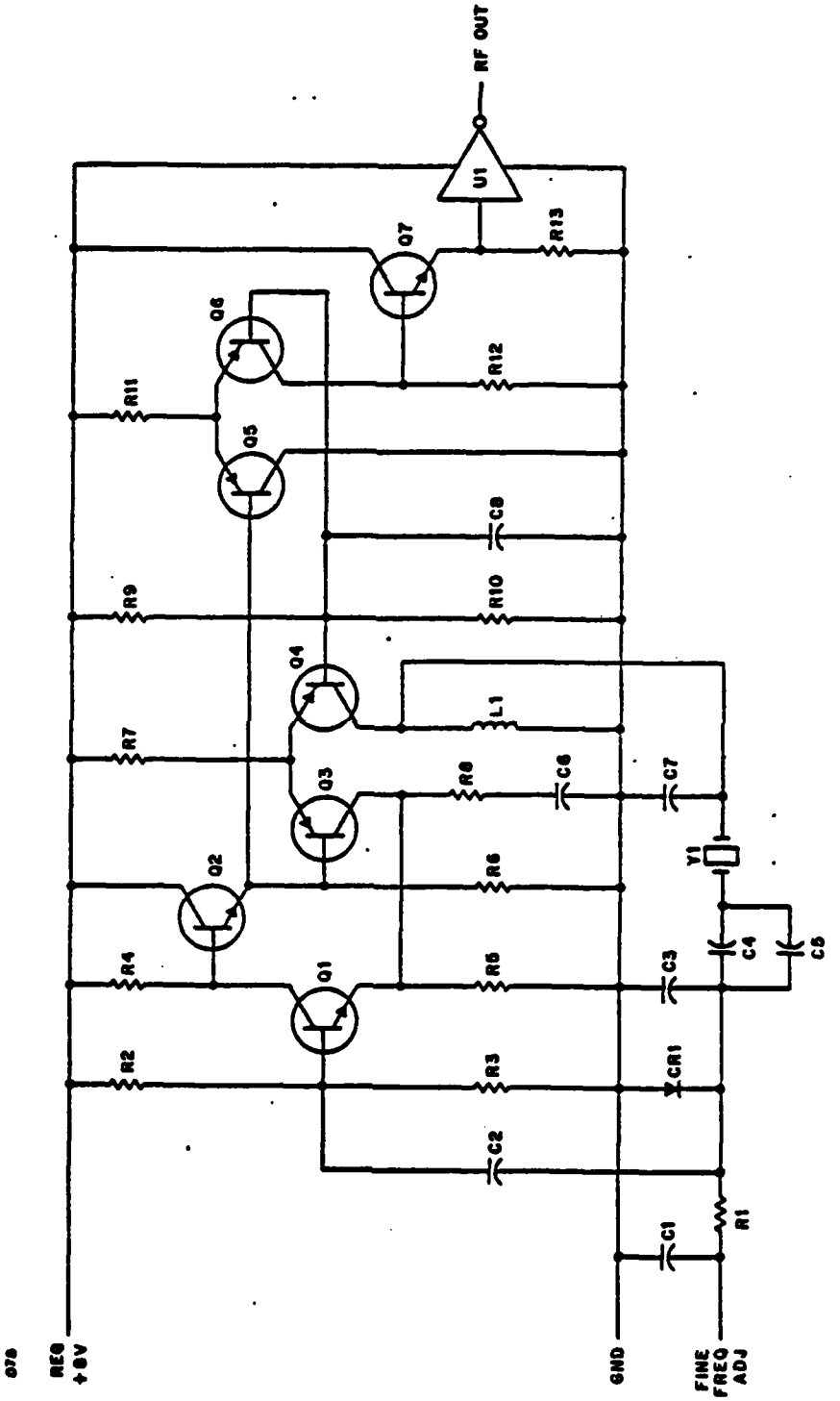

FIGURE 2-3 - SELF LIMITING OSCILLATOR CIRCUIT

In this circuit, differential amplifiers Q3/Q4 form a limiter whose output peak to peak current is limited to the quiescent current through R7. This current value, in conjunction with matching elements L1 and C7 determine the crystal current. The crystal current, flowing through C3 and CR1 in parallel, provide an input voltage to amplifier Q1 which is well within its linear operating region, with the result that the crystal sees constant drive current and constant terminating loads. Differential amplifier Q5/Q6 and amplifiers Q7 and U1 provide load isolation.

Several oscillator circuits in combination with the ceramic enclosed crystal units will be evaluated for compliance with specification requirements.

(3) TEMPERATURE CONTROLLER. The temperature control circuit used in the current TMXO design is shown in Figure 2-4. This circuit consists of a resistance bridge containing a thermistor, a proportional plus integral amplifier, and a heater. It has been tested in several different microcircuit configurations with excellent results. Therefore, there is no obvious reason to modify the circuit configuration. However, limits on long and short term drift will be established and worst case analysis will be performed. Particular attention will be given to thermistor stability and drift and to the leakage current in the integrating capacitor C1.

Additionally, in conjunction with thermal analysis, transistor size, location and quantity will be determined.

(4) VOLTAGE REGULATOR. The existing voltage regulator circuit is shown in Figure 2-5. It has also been used extensively in the TMXO application with satisfactory results. The circuit consists of a reference diode, constant current bias diode, and an isolation amplifier.

Problems observed with the circuit have principally been caused by noisy reference diodes or noisy operational amplifiers. These problems will be eliminated in production by properly specifying the components, and by screening. As with the other circuits, a worst case design analysis will be performed.

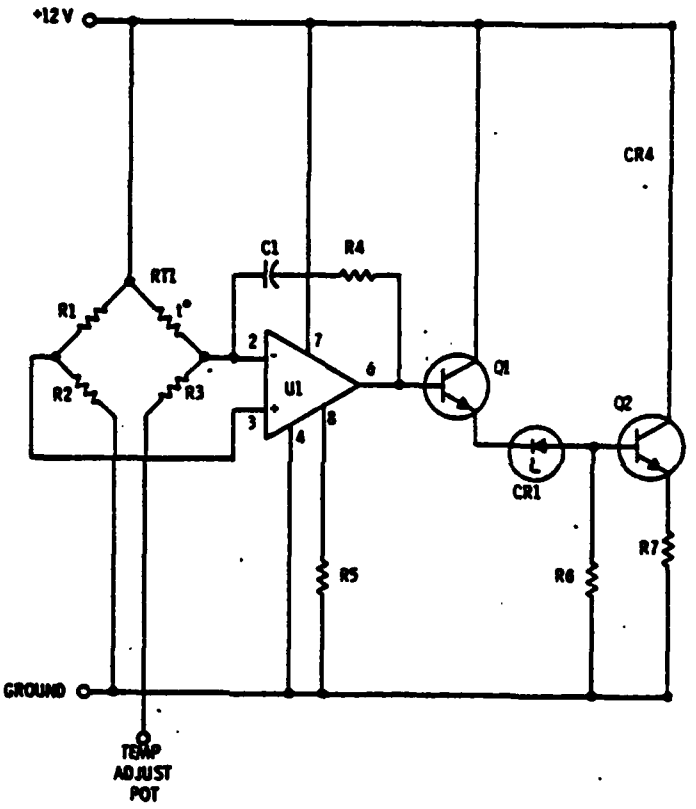

FIGURE 2-4 - THERMAL CONTROL CIRCUIT

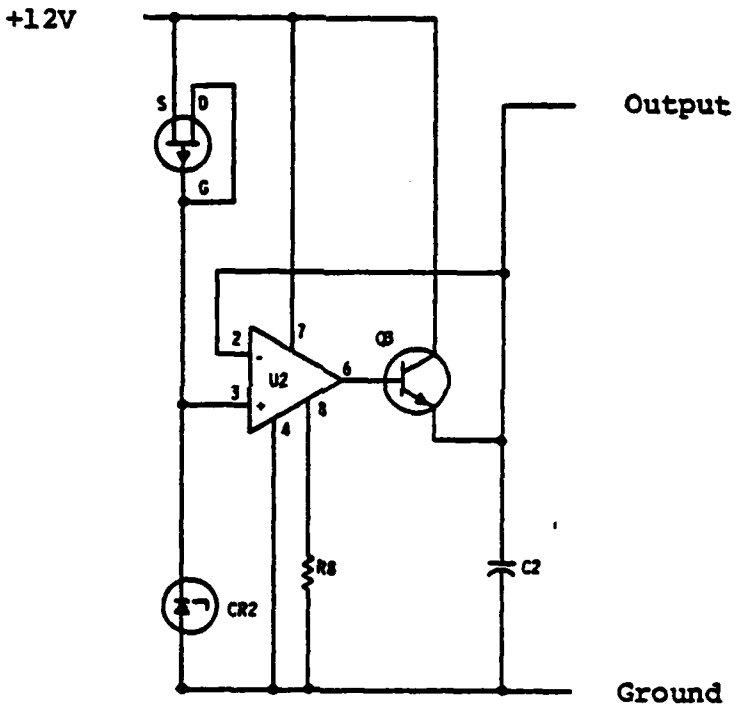

FIGURE 2-5 - VOLTAGE REGULATOR

(5) BUFFER AMPLIFIER. The design of the buffer amplifier will depend on the final configuration of the oscillator circuit. No significant difficulties are anticipated in the design of this circuit.

2B MECHANICAL DESIGN

(1) GENERAL. Two mechanical design considerations require particular attention to optimize oscillator performance. First and foremost, is the maintenance of low thermal losses required for temperature stability and low total power operation. The second involves stability in shock and vibration environments.

Low thermal losses are achieved by mounting the crystal/microcircuit assembly on a thermally isolating pedestal within the vacuum of an outer enclosure, thereby minimizing heat flow out of the oscillator assembly. Of primary importance in maintaining low thermal losses is the maintenance of the vacuum, which evolves into three considerations. First, and most obvious, is the reliability of the hermetic seal between the vacuum and the outside atmosphere. Second is the hermetic seal reliability of the crystal and microcircuit packages whose internal pressures are several magnitudes below atmospheric, but still above that of the surrounding vacuum. The third vacuum maintaining consideration is the minimization of post seal outgassing from materials within the vacuum area. Outgasses, if unabsorbed, can cause vacuum pressure increase. By limiting outgas to a low rate, gas absorbing getter material inside the TMXO will prevent vacuum pressure buildup. High seal reliability and low outgassing characteristics guarantee low TMXO heat loss thereby limiting operating power requirements at $-54^{\circ}C$ to 250 milliwatts and power aging to 1 percent per month.

Particular emphasis is given to this foremost task of sealing the TMXO by production methods and in production type facilities. New materials, processes and techniques require investigation and review for application to the volume production of highly reliable TMXO assemblies.

The second important area of TMXO mechanical design consideration is that of frequency stability in shock and vibration

environments. An oscillator assembly designed for wide usage application will undoubtedly be exposed to high shock and vibration environments in many tactical applications. By its nature, crystal performance is dependent upon its ability to move or vibrate in a prescribed manner, the restriction or modification of which can cause an adverse affect. The TMXO crystal and microcircuit packages are mounted on a support pedestal for thermal reasons previously discussed. For stability under shock and vibration conditions the support system is designed for the high rigidity necessary to prevent the introduction of undesired motion. The support structure is proportioned to provide stiffness while giving complete consideration to maintaining a high thermal resistance.

(2) OVERALL CONFIGURATION. The TMXO consists of five basic mechanical assemblies, which are (1) the header, (2) the cover, (3) the thermal isolating pedestal, (4) the microcircuit assembly, and (5) the crystal assembly, as shown in Figure 2-6.

The crystal assembly is solder attached to the microcircuit assembly which is secured to a mounting plate. The entire crystal/microcircuit assembly is mounted to the pedestal with screws in the four corners. Prior to attachment of the crystal/microcircuit assembly, the pedestal is secured to the header with screws in its base. Six ceramic to metal feedthroughs are provided in the header for electrical connection to the oscillator assembly. Two more feedthroughs are provided in the header cavity. The cavity is formed integrally into the header to provide convenient location for and access to the temperature setting potentiometer. The outer enclosure cover seals around its periphery to the header and is equipped with an oxygen free high conductivity (OFHC) tubulation. The tubulation provides a means in production application for connecting multiple oscillators to the vacuum manifold outside the vacuum chamber for convenient test, and outgas bake, after which the tubulation is pinched-off and then solder sealed to maintain high hermeticity. The tubulation will be approximately 0.25 + 0.50 inches in length after sealing.

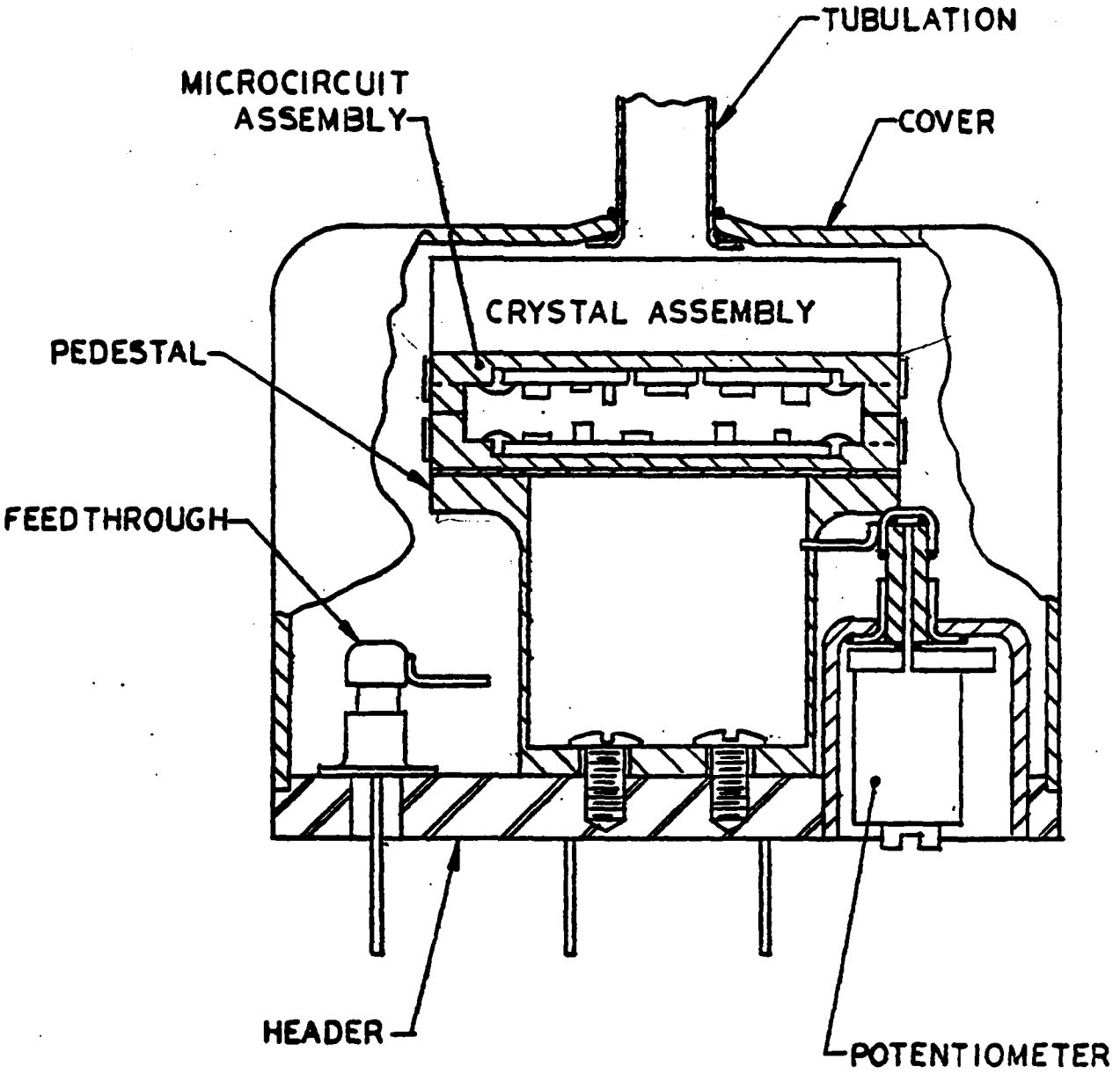

FIGURE 2-6 - OVERALL CONFIGURATION

Pedestal design considerations are primarily to provide support for the crystal/microcircuit assembly while providing high thermal resistance to minimize heat conduction to the header.

Microcircuit package outline configuration is identical to the octagon shaped crystal package. Both are of ceramic material with metallization on the interfacing surfaces whereby they are soldered together prior to assembly to the pedestal. A drawing of the basic microcircuit package is shown in Figure 2-7. The cavity within the package is .105 deep providing depth for the microcircuit substrate (approximately .015 thick) and the maximum height chip component (.07). A step area around the inside of the cavity is locally metallized at each of the octagon flat sides to provide conductive path feedthroughs fired-in when the ceramic package is cured. The feedthroughs are connected to the sides of the package by metallization to which the lead wires are brazed. The final microcircuit package is assembled by sealing the tops of two such packages together with substrates inside each. The heater circuitry with the centrally located heater is located in the top half for proximity and symmetry with the crystal.

(3) THERMAL DESIGN. Thermal design of the TMXO involves two separate aspects. The first is to minimize the heat loss from the oscillator to require not more than 250 milliwatts operating power at any temperature between -54° to $+75^{\circ}$C. The second is to minimize temperature gradients within the crystal.

Heat loss from the oscillator is limited by the following methods:

(a) Placing the crystal/microcircuit assembly in a vacuum (1×10^{-4} Torr) to eliminate all gaseous conduction and convection.

(b) Providing a high thermal resistance support pedestal. The pedestal material is polyimide plastic-Dupont's VESPEL SP-1. The pedestal thermal resistance is approximately 1800° C/W.

(c) Selecting lead wires with high thermal to electrical resistivity ratios. Some materials with high ratios are

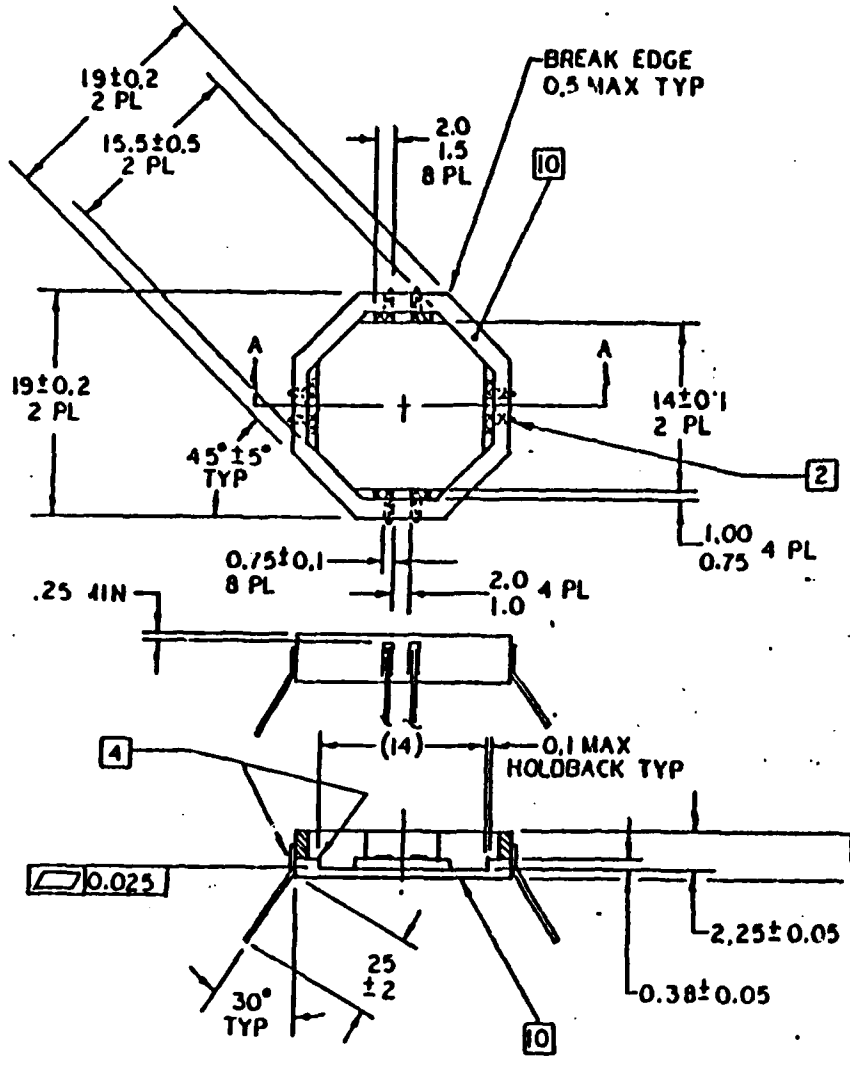

NOTES:

1. MATERIAL: BODY: BERYLLIA (99.5% BEO)
   LEADS: 10 MIL DIA NICKLE
2. INDICATED AREA TO BE TUNSTEN METALLIZED THRU FROM INSIDE TO OUTSIDE. CONFIGURATION OF FEEDTHRU PORTION OPTIONAL.
3. LEADS AND BRAZE PADS TO BE PLATED IN ACCORDANCE WITH THE REQUIREMENTS OF MIL-M-38510.
4. FOLLOWING FABRICATION AND PLATING, RESISTANCE OF FEED-THRU INCLUDING BRAZED JOINT TO BE LESS THAN .05 OHM.
5. UNLESS OTHERWISE SPECIFIED. ALL DIMENSIONS ARE IN MILLIMETERS.
6. ASSEMBLY SHALL BE LEAK CHECKED WITH EQUIPMENT CAPABLE OF DETECTING LEAKS AS LON AS 1×10-12 STD CC'S/SEC. ASSEMBLY SHALL SHOW NO INDICATION OF A LEAK.
7. FLATNESS OF CERAMIC TO BE .1/25 MM.
8. LEADS SHALL WITHSTAND A PULL TEST OF 340 GRAMS MINIMUM APPLIED ALONG THE CENTERLINE OF THE LEAD AT AN ANGLE OF 15° ± 5° OUTWARD FROM ITS NORMAL POSITION.
9. PACKAGE SHALL MEET ALL REQUIREMENTS OF MIL-M-38510 LEVEL B.
10. TUNGSTEN METALLIZED SURFACE PLATED GOLD PER MIL-M-38510
11. LEAKAGE FROM EACH LEAD TO ALL OTHER LEADS SHALL NOT EXCEED 5 NA @ 100 VDC.
12. CAPACITANCE BETWEEN MUTUALLY INSULATED CONDUCTORS SHALL NOT EXCEED 5 pf AT A TEST FREQUENCY OF 1000 Hz.

FIGURE 2-7. 8 LEAD PKG SIDE BRAZED

Silver (114), Nickel (112), Gold (111), Tantalum (104), and Palladium (101). One or more are used as determined by other requirements, such as strength, attachment means, etc.

(d) Polishing the inside of the cover to present a highly reflective surface to the radiant energy discharge from the crystal/microcircuit assembly. Any radiant energy not reflected by the inside of the cover is absorbed thereby heating the cover and eventually giving up its heat to the surrounding medium.

Temperature gradients within the crystal are minimized by the following methods:

(a) Symmetry - The heater is placed in the center of the package and mass densities are placed symmetrically.

(b) High conductivity materials are used for low resistance to heat flow. The microcircuit package material is Beryllia (99.5% BeO) with thermal conductivity of 214 mils ^{o}C/watt (Aluminum is 192). A copper package could be considered here; however other considerations such as plating and ceramic-to-metal feedthrough requirements reduce copper's advantage.

(c) Back-filling the crystal enclosure with Nitrogen to assist thermal distribution and rapid warm-up.

(d) Thermally conductive epoxies for hybrid chip mounting.

The warm-up characteristics for a temperature controlled substrate and enclosure are determined by the energy (H) that is required to heat the mass to the desired temperature given by:

$$H = 4.186 [c(Ts - T_A) V]$$

where H is expressed in watt-seconds

C is the thermal capacity of the mass in cal/cm^3 ^{o}C

V is the total mass volume in cubic centimeters

For both the crystal and microelectronics enclosures

$$H = 4.186 [.86 (89 + 54) 1.42]$$

$$H = 731 \text{ w sec}$$

With 10 watts at -54^{o}C enclosures will be at temperature in 73 secs. To be within $\pm 1 \times 10^{-8}$ of final frequency in three

minutes, there is one minute and 47 seconds for the crystal to stabilize from its overshoot.

(4) SEALS AND VACUUM TECHNIQUES. Of primary importance in the mechanical design of the TMXO is maintaining the vacuum within the enclosure. For acceptable thermal performance over a long period the pressure within the TMXO must not increase above 1×10^{-4} Torr which depends on several things: first, the external seals; second, the internal package seals; and third, the outgas characteristics.

The ceramic to metal feedthroughs used in the header are a production item brazed to the header and have demonstrated leak integrity. The final closure seal between the cover and the header is a low temperature solder joint since the crystal/ microelectronic package should not be exposed to temperatures over 180°C. The final pinch-off of the tubulation is done with special tooling to keep the extension as short as possible and is immediately sealed with solder. After final seal the tubulation will be protected by a cap and the feedthroughs will be protected by filling the cavities with epoxy. Extensive investigations will be performed to determine the availability of other type feedthroughs and other methods of making the final closure such as laser or electron beam welding where the heat can be restricted to the joint area.

The internal package seal has been limited to one solder seal as explained in paragraph 2.2.2 by sealing two open top microcircuit packages together at their metallized interface by inverting one on top of the other. This solder joint will be made at a higher temperature than the final seal at about 240°C so that the microcircuit package and crystal package can be joineed at approximately 200°C. The electrical feedthroughs in the microcircuit package are metallized onto the green ceramic and fired-in-place when the package is made, providing a very reliable feedthrough method.

Outgassing of materials in vacuum is a result of several actions. If the material involved has a high vapor pressure molecules of vapor will tend to escape in low pressure atmosphere

especially if the material is heated. Materials with high vapor pressure, say above 1×10^{-11} such as zinc or tellurium will have a tendency to cause a pressure buildup in a vacuum and are to be avoided. Non metals are even more suspect and will be investigated thoroughly before usage. All materials have absorbed gases and most materials have absorbed gases as well, which escape from the surface when exposed to a high vacuum environment. Since outgassing is proportional to the exposed area it is advantageous to have smooth highly polished surfaces rather than rough ones.

By investigating improved outgas techniques, by selecting the proper materials and finishes, and by performing vacuum outgassing and bakeout prior to sealing, the outgassing characteristics are maintained below that of the getter capability for long term vacuum performance.

(5) MATERIALS AND FINISHES. The following materials are being used in the TMXO:

The TMXO Cover - Monel Ally 400 is a nickel-copper alloy. Stainless steel and Kovar are also being considered for this application .

The Tubulation - Oxygen Free High Conductivity (OFHC) Cover.

The TMXO Header - Same as the TMXO Cover.

The Header Feedthroughs - Kovar and Nickel.

The Support Pedestal - Polyimide - Dupont's Vespel SP-1.

The Microcircuit Support Plate - Nickel.

The Microcircuit Package - Beryllia (99 .5% BeO).

Material selection is made with consideration given mainly to vacuum performance, corrosion resistance without plating and joining capability.

Additional finishes such as platings and coatings are suspect in a high vacuum environment since gases and liquids can become trapped under coatings. It may become necessary to plate some parts to be able to join dissimilar metals but platings could be restricted to the joint area.

(6) SHOCK AND VIBRATION. Acceleration, shock and vibration are of all one general category and reflect the rigidity of the support system, mainly the pedestal. Pedestal design has been

proportioned to provide a high thermal resistance while maintaining the theoretical natural frequency above 500 Hz since some applications of the TMXO will experience vibrations to 500 Hz. The system can be treated as an end loaded cantilevered beam with the pedestal acting as the beam and the crystal/microcircuit assembly as the end load. The equation for the resonant frequency in the bending mode is:

$$f_n = \frac{1}{2\pi} \sqrt{\frac{K}{N + .23m}} \text{ Hz}$$

n is the end loaded mass
m is the beam mass
K is the beam spring rate

where $K = \frac{3EI}{L^3}$

E = modulus of elasticity
I = moment of inertia about the spring axis
L = beam length

then

$$f_n = \frac{1}{2\pi L} \sqrt{\frac{3EI}{L(n + .23m)}} \text{ Hz}$$

With pedestal wall thickness equal to .0125 inch the natural frequency is greater than 500 Hz.

3. PLAN

Due to the critical and interacting nature of various components and techniques used in the TMXO, the planned efforts during this reporting period were to be directed toward optimization of components, techniques and analysis.

3A CIRCUIT, CRYSTAL AND COMPONENT EVALUATION. To effectively evaluate crystals, circuits and components, a number of precision environmentally controlled test bed articles are required. The test bed should provide temperature stability better than 1 millidegree over periods of hours, with temperature adjustability over the anticipated range of crystal turn temperatures. The test bed should provide a high stability voltage source for energizing test oscillators, and volume sufficient to accommodate complete TMXO assemblies or portions thereof.

In order to evaluate crystal retrace and aging, a facility must be provided with sufficient resolution capability, but having a small facility aging/retrace contribution. Our plan is to develop an oscillator circuit having essentially no reactance elements which contribute to the frequency of oscillation of the crystal under test. The oscillator and candidate crystals will then be subjected to the retrace temperature profile and long term operation to characterize crystal retrace and aging.

Once the facility has been operated to characterize a crystal, means will be provided to allow the introduction of test reactive elements into the crystal circuit. The subsequent change in performance will allow deduction of the characterization of the candidate reactive elements to the required accuracy. This required accuracy is far greater than that obtainable from commercially available component evaluation devices such as bridges, etc., to determine component characteristics not adequately specified by the supplier, such as flicker noise in operational amplifiers and voltage regulators for example.

3B PACKAGING. Success of the TMXO thermally, and as a result, frequency stability is highly dependent on the sealing techniques and materials selected to allow a high vacuum to be realized and

maintained. A study of baseline and alternate materials, techniques and configuration was envisioned.

3C THERMAL ANALYSIS. Due to the extremely low power, crystal temperature criticality and large temperature difference between the crystal and the environment, and due to the impracticability of preliminary testing, a thermal analysis of the system was envisioned. This analysis was to start with a course analysis of the baseline system and expanded, as needed, to allow exact solutions of thermal losses, temperatures, and warm-up time.

4. ACCOMPLISHMENTS

A number of the planned objectives were satisfied during this reporting period and some of the original base-line approaches were changed as a result of investigative efforts. The accomplishments and the new directions taken are described in the following results.

4A SPECIAL TEST FACILITIES. Special test facilities have been developed to aid in the evaluation of crystals, components and circuits. The equipments are described below.

(1) LABORATORY TEST BED. A carefully designed laboratory test bed is necessary for evaluation of circuits, crystals, and other components. The laboratory test bed must have a mechanical configuration which is consistent with precision temperature control while providng for convenience in replacing various circuit elements and components which are to be evaluated.

The basic test bed enclosure (oven) consists of an aluminum tube with a cap at each end. Channels are provided in the outside surface of the tube for mounting temperature sensors (thermistors) which are used for monitoring and control. The tube is heated with resistance wire tightly wound around the outside from end to end.

The electronic components are mounted on circular printed wiring boards supported in a fashion similar to that used in a standard wafer switch. This multiple wafer assembly is placed inside the aluminum tube and the end caps are attached. Electrical connections are made via a multi-conductor cable assembly which passes through one end cap.

The entire assembly is placed inside a Dewar flask which provides thermal insulation. This reduces the effects of environmental temperature changes and reduces heater power consumption.

The ratio of the change in ambient temperature to change in oven temperature (gain) is a good measure of the effectiveness of the system. It is desirable to use the maximum gain possible consistent with stability of the control system. The achievable gain is a function of several parameters including the thermal

resistance from the oven assembly to the ambient, the response time of the thermistors, and the thermal capacity of the oven. These parameters are identified as follows:

Oven Chamber Size	2" Dia. x 2.5" Length
Thermal Leakage Resistance	54°C/Watt
Thermal Capacity	280 Watt Sec/°C
Time Constant (Uncontrolled)	4.2 Hours

The maximum value of stable gain was determined by first measuring the impulse response of the oven/thermistor composite assembly. This impulse response was then used to synthesize a resistor - capacitor electrical analog of the thermal circuit. Using this electrical analog, it was then possible to perform a computer simulation of the system using the gain of the amplifier as a variable parameter. With this technique, the optimum value of amplifier gain was determined.

A schematic diagram of the final oven control circuit is shown in Figure 4-1. The circuit consists of a resistance bridge containing the thermistor, an amplifier stage U1a, and a heater circuit consisting of U1b, Q1, Q2, and associated resistors. The current through the heater resistance is supplied by transistor Q2 which is external to the oven assembly. Since Q2 is in an uncontrolled environment, negative feedback to the inverting input of U1b is used to eliminate any effects of parameter changes in Q2 resulting from ambient temperature fluctuations.

The gain of the system is given by the following expressions:

$G = 2 K_t K_a g_h R_t V$

Where K_t = sensitivity of thermistor bridge in volts/°C

K_a = gain of amplifier

g_h = conductance of heater resistor

R_t = thermal resistance from oven to ambient

V = voltage applied to heater resistance

Since these parameters are known or can be easily measured, calculation of system gain is straight forward. For the system under consideration, the gain is equal to 1200.

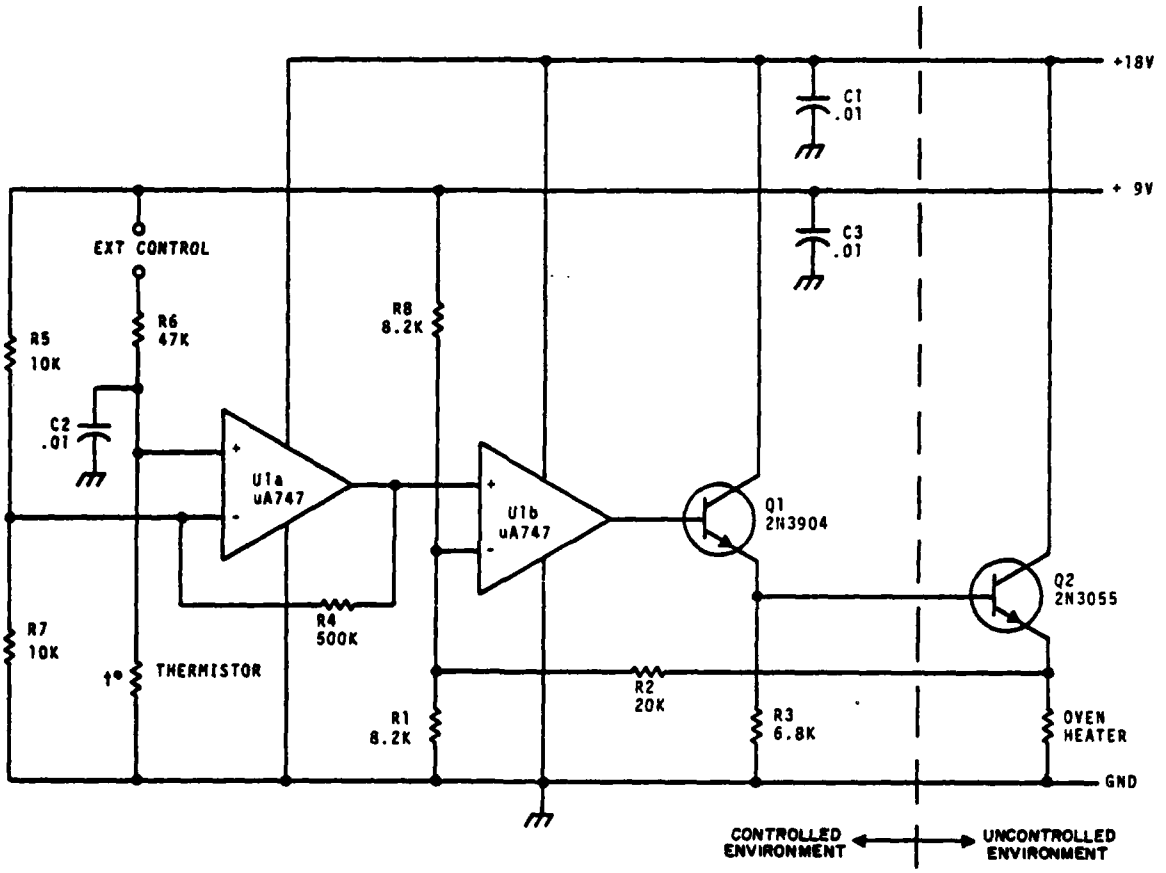

FIGURE 4-1 - TEST BED OVEN CONTROL CIRCUIT

The Test Bed includes a voltage regulator subassembly, which provides a stable supply for the oven control circuit and for test oscillators to be evaluated in the Test Bed.

The voltage regulator circuit is shown in Figure 4-2. The circuit is similar to the circuit previously used in the TMXO except for the addition of chokes to prevent RF coupling through the regulator common impedance. Filter components L1 and C1 were also added to eliminate the higher frequency components of the zener noise. The use of a 6.4 volt zener makes it necessary to obtain some amplification of the zener output to provide a regulator output of 9 volts. This gain is determined by resistors R3 and R4. The bias current for the zener diode is supplied by constant current diode CR2.

Performance of the complete test oscillator assembly with respect to ambient temperature change is shown in Figure 4-3. The ambient temperature was changed from $+20^{\circ}C$ to $-40^{\circ}C$ which produced an oven temperature change of approximately $.055^{\circ}C$. The frequency change following an initial transient overshoot was approximately .013 Hz or a relative change in frequency of 2.5×10^{-9}.

The transient response of the thermal control circuit is illustrated in Figure 4-4. The vertical axis represents the change in the monitoring thermistor resistance while the horizontal axis represents time. Samples were taken in .4 second increments. The sensitivity of the vertical scale is approximately 4 ohms per millidegree. The curve represents the response of the oven near the end of a 5 degree step in control temperature.

(2) PHASE PERTURBATION EVALUATION TEST FACILITY. One area of performance requiring further investigation is the short term stability of the oscillators, particularly when measured over time intervals in excess of 10 seconds. While the stability over a one second interval is satisfactory, a degradation is observed over longer intervals. The perturbations appear to have the charcteristics of flicker noise; increasing amplitudes corresponding to lower perturbation frequencies.

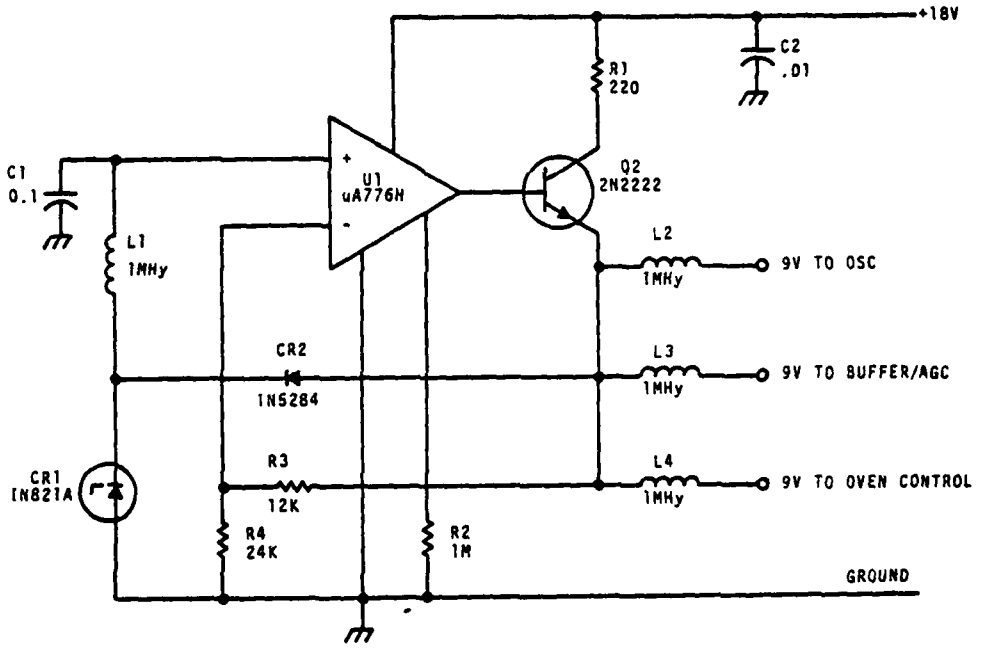

FIGURE 4-2 - TEST OSCILLATOR VOLTAGE REGULATOR

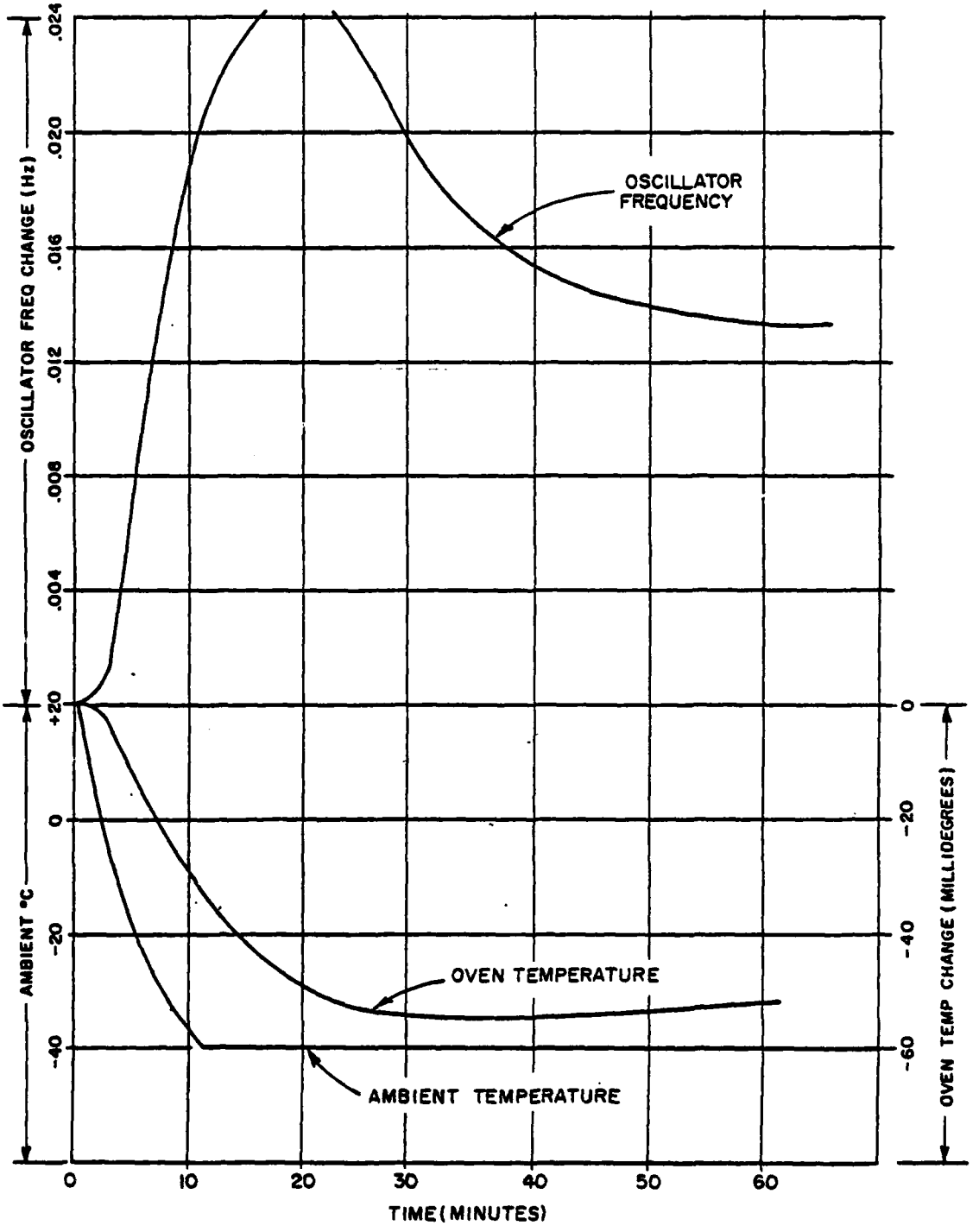

FIGURE 4-3. TEST OSCILLATOR ASSEMBLY AMBIENT TEMP VS. TIME VS. FREQUENCY

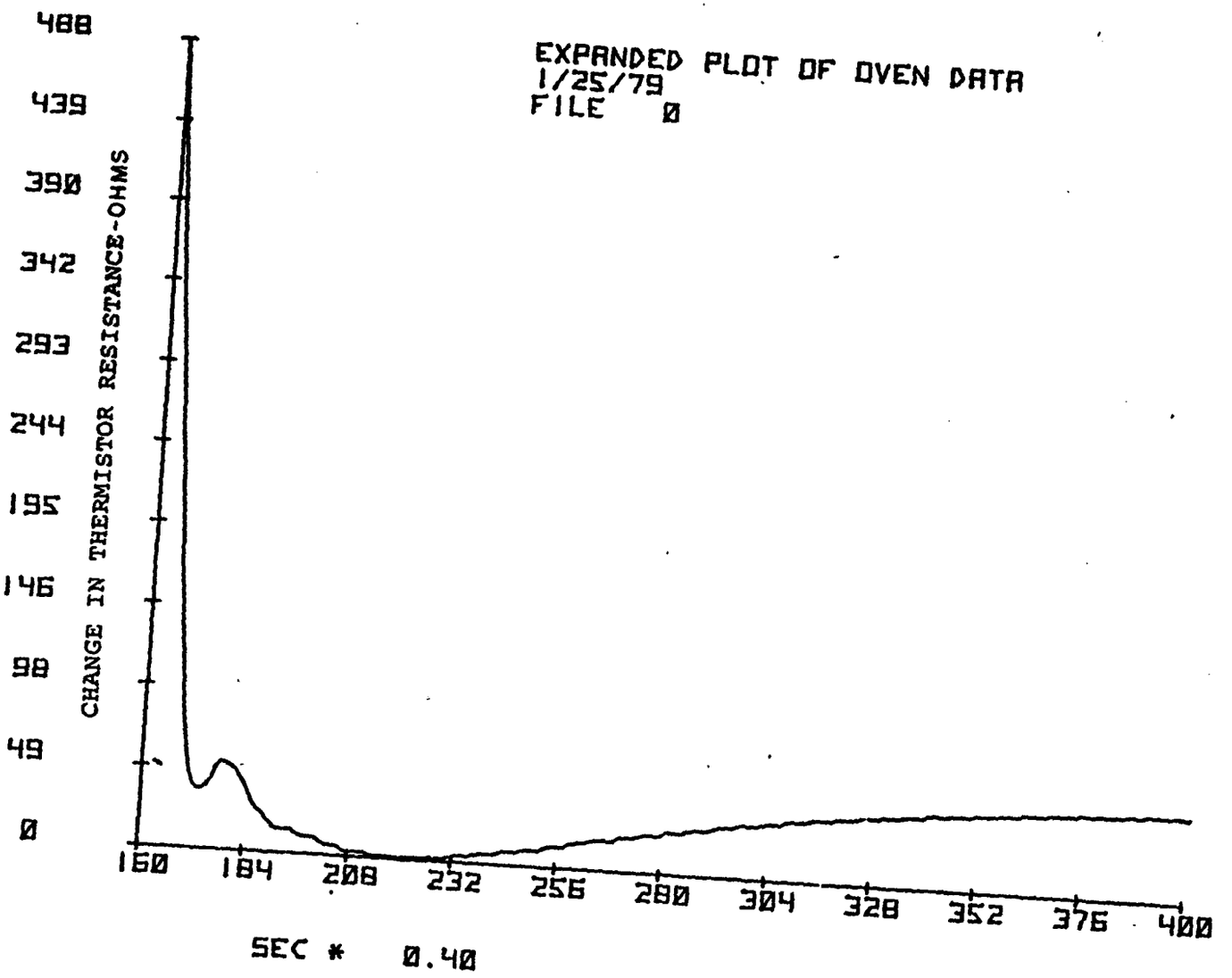

FIGURE 4-4. EXPANDED PLOT OF OVEN DATA

In a closed loop oscillator circuit, it is difficult to isolate and characterize the sources of these low frequency perturbations.

An effort is being made to measure, independent of test oscillators, the low frequency phase perturbation associated with circuit elements and components. An implementation of a facility for these measurements is shown in Figure 4-5. A highly phase-stable source is divided into direct and quadrature components by a 90 degree hybrid. The device under evaluation (crystal, amplifier, etc.) is inserted into one path. The length of the other path is selected to present quadrature inputs to the mixer, with the direct component of the mixer output representing the differential phase.

The operating signal level provides a gradient of the order of 1 volt/radian, or 1 volt per micro-radian. The phase analog signal is fed to a low noise amplifier contributing <1 μvolt peak to peak (P/P) over periods from 1 second to 1 minute. The phase stability implied by the oscillator specification of frequency stability is as follows: a short term stability of $\Delta F/F = 1 \times 10^{-11}$ @ F $\approx$5 MHz requires $\Delta F(RMS) < 50 \times 10^{-6}$ Hz. With $\pi/2$ radians phase change over a 10 Hz crystal 3 dB bandwidth, $\Delta F/\Delta\phi \approx 6.4$ Hz/radian, resulting in phase perturbations

$$\Delta\phi < \frac{50 \times 10^{-6}}{6.4} = 8\ \mu \text{ radians RMS}$$

The phase perturbation resolution of the facility is therefore about an order of magnitude better than the specification limit.

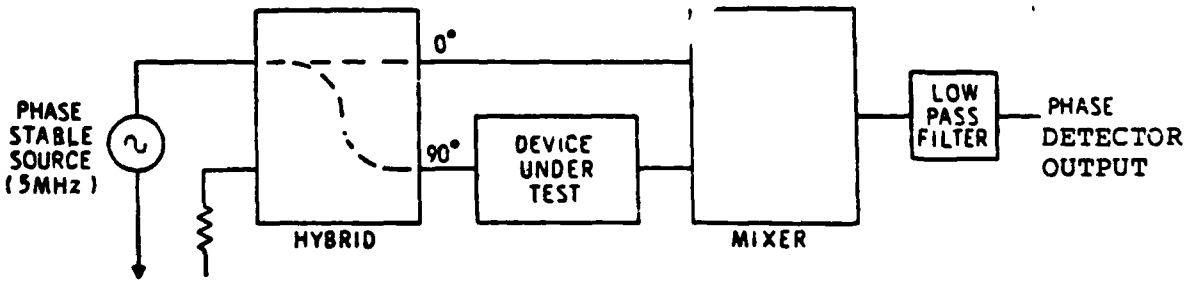

FIGURE 4-5 - PHASE PERTURBATION MEASUREMENT FACILITY

To date, preliminary evaluation of the Test Bed buffer amplifier, and the active portion of the test oscillator and buffer amplifier have been evaluated and found to contribute negligible phase perturbation within the frequency band described. Future work will evaluate the phase stability of crystals and the possible perturbation of the crystal resonant circuit attributable to input and output load variations of the active portions of the oscillator circuit.

(3) OUTGASSING TEST CHAMBER. Bendix Research Laboratories has manufactured an outgassing test chamber. Investigation of the characteristics of the chamber are still underway; however, some initial data has been obtained. The chamber will be used to evaluate candidate materials and processes for excessive outgassing and to determine proper pretreatments of materials to reduce outgassing.

4B ELECTRONIC DESIGN

(1) CRYSTAL/OSCILLATOR CIRCUIT EVALUATION. Two new oscillator circuits have been designed for use in crystal and component evaluation.

(a) TEST OSCILLATOR FOR CRYSTAL RETRACE/STABILITY MEASUREMENTS. Temperature cycling of crystal oscillators can produce significant permanent change in operating frequency. It would be highly desirable to be able to separate frequency change attributable to the crystal from changes due to other circuit components. With this in mind, a new series mode circuit was developed which is essentially free of any reactive components which might contribute to frequency shift after thermal cycling.

The basic idea of the circuit is to provide a purely resistive termination for the crystal. This terminating resistance is made as small as possible so as not to reduce the circuit Q significantly.

The circuit consists of a two transistor amplifier having unity voltage gain but very low output resistance. The output of this amplifier drives one terminal of the crystal. The second terminal of the crystal is connected to the input of another two transistor amplifier having unity current gain and low input

resistance. The output current of the second amplifier is applied to a load resistor. The total gain from the input of the first amplifier to the load resistor of the second amplifier is approximately equal to the ratio of the load resistor to the equivalent series resistance of the crystal.

The phase shift through the circuit is very small and if the output is connected to the input, oscillation will result, if the gain is greater than unity. In the actual circuit, a field effect transistor connects the output to the input so that automatic gain control (AGC) can be used to control the level of oscillation.

Since the circuit has no frequency determining elements other than the crystal, the circuit would not generally be useful in evaluating overtone crystals unless the series resistance is lowest at the desired overtone. However, if fundamental crystals can be characterized for frequency retrace and if the effects are predictable, then other components such as inductors and capacitors can be evaluated by inserting them into the crystal circuit.

A schematic of the oscillator circuit is shown in Figure 4-6.

The AGC amplifier/detector circuit is shown in Figure 4-7. The circuit consists of a three transistor feedback amplifier (Q2, Q3, Q4), output buffer transistor Q1, and a detector containing diodes CR1 and CR2. The gain of the feedback amplifier is determined by resistors R5 and R6 and is equal to approximately 100. The signal level at the output of the amplifier with the AGC loop closed is approximately 2 volts pp.

(b) SELF LIMITING OSCILLATOR. An alternate design for a self-limiting oscillator is being evaluated. The circuit is shown in Figure 4-8.

The compound amplifier Q2/Q3 drives amplifier Q4 in a cascade configuration, with a voltage gain determined by the ratio of Q4 collector load to crystal impedance. The quiescent current established by source Q1 is chosen to allow Q2/Q3 to present a low impedance to the crystal, to maintain high circuit Q. Differential pair Q5/Q6 operate as a limiter to maintain constant drive to Q2 input to complete the oscillator loop.

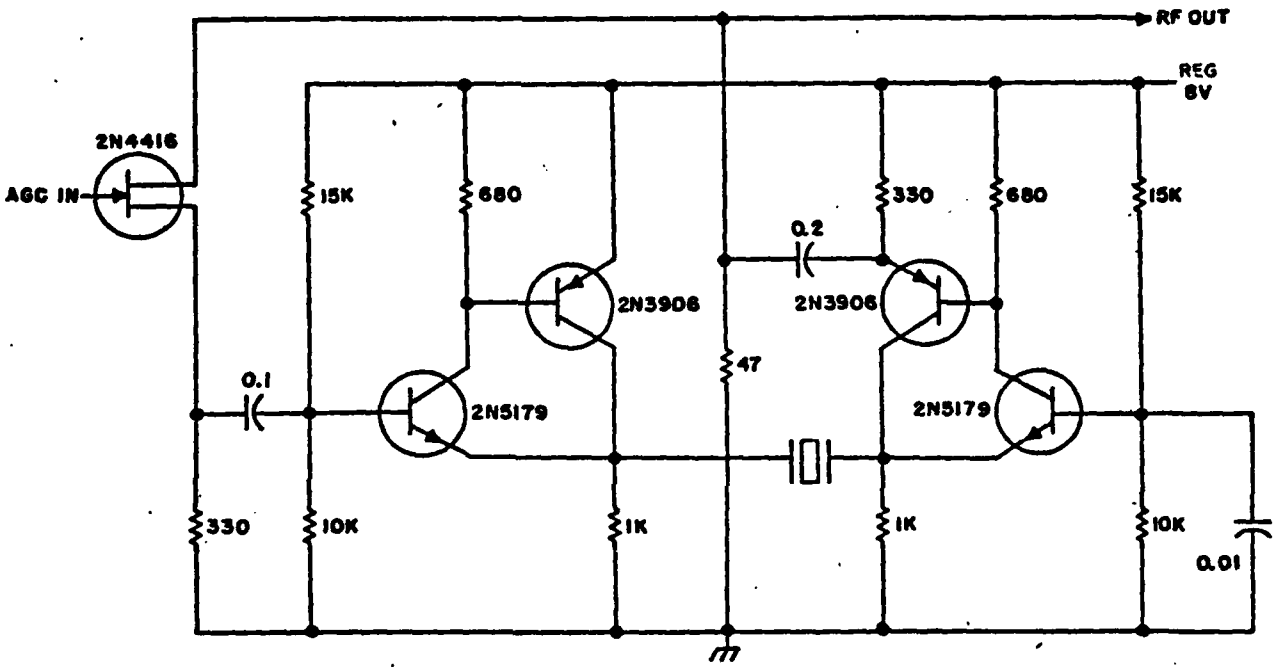

FIGURE 4-6 SCHEMATIC DIAGRAM OF SERIES MODE OSCILLATOR CIRCUIT

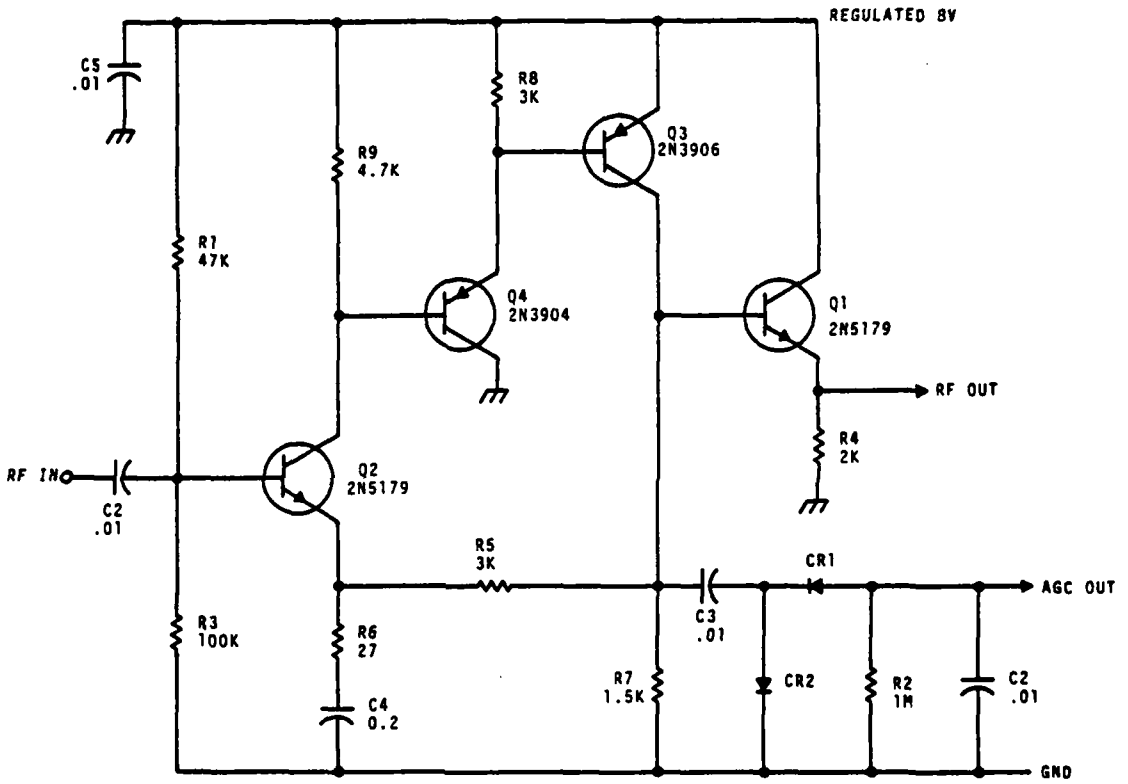

FIGURE 4-7. AGC AMPLIFIER/DETECTOR

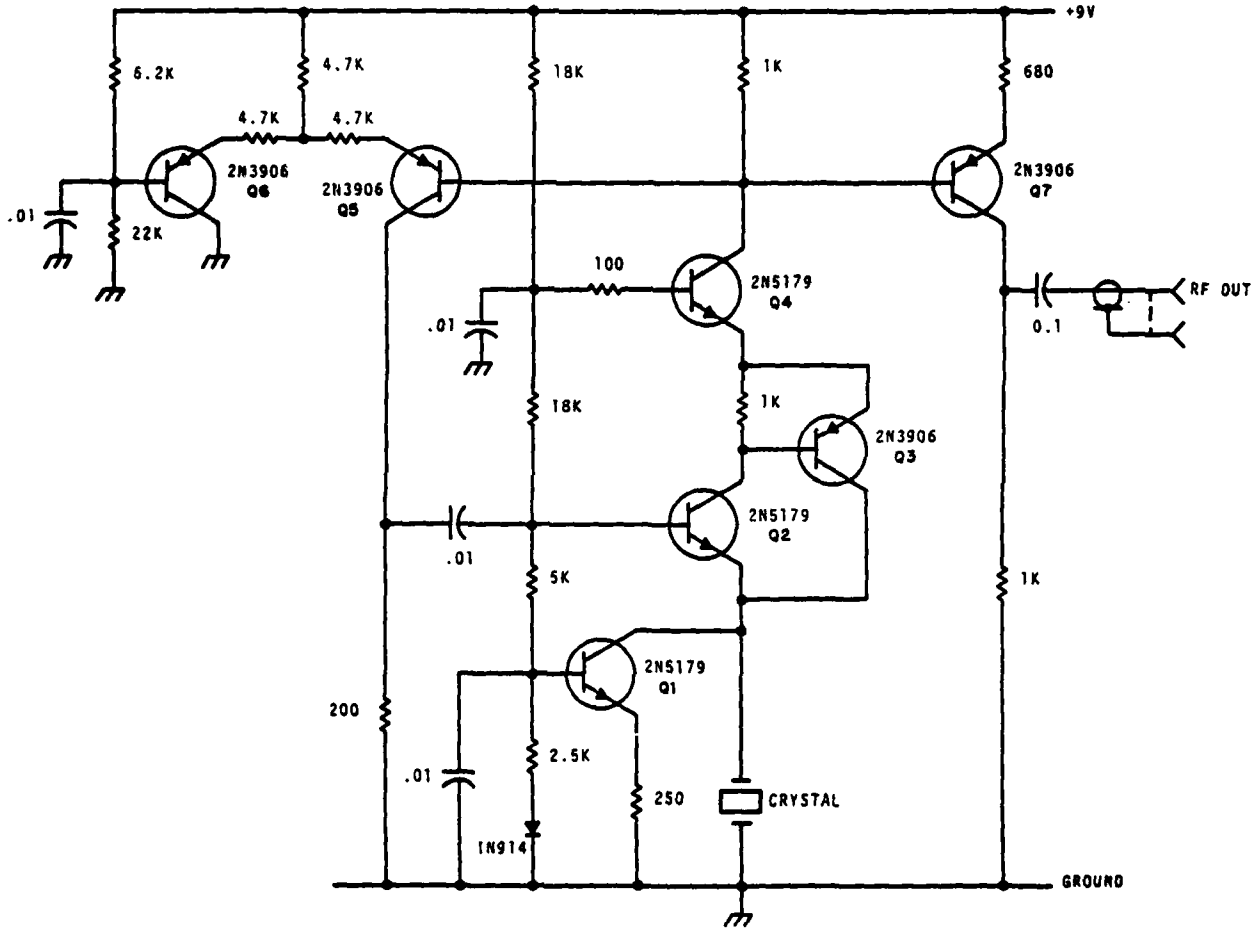

FIGURE 4-8. ALTERNATIVE OSCILLATOR DESIGN

A high level signal with essentially full crystal selectivity is available to drive the isolation amplifier Q7 at near unity gain.

This oscillator has been used primarily to compare short-term stability among crystals, as described in paragraph 4.2.2.

(2) CRYSTAL EVALUATION

(a) PARAMETER VALIDATION. Crystal parameters were measured on the crystal impedance meter. The motional capacity and series resistance of all 5.115 MHz units were closely grouped about C_1 = 0.01 pF and R_{s1} = 6 ohms.

(b) SERIES RESISTANCE TEMPERATURE DEPENDENCE. The dependence of crystal effective series resistance on temperature was evaluated. The result was only slight variation of resistance from room temperature to the upper turn temperature.

(c) PRELIMINARY AGING RATE MEASUREMENT. One of the ceramic package crystals was placed in the test circuit described in paragraph 4.2.1.1 for preliminary evaluation. Initial results of crystal performance were encouraging.

A record of the performance of crystal #157 in the test oscillator circuit is shown in Figure 4-9. The record starts shortly after turn-on and continues for about 20 hours thereafter. The horizontal scale is 1 inch/hour and the vertical scale is .01 Hz/inch. The crystal current was adjusted to approximately 50 microamps which is equivalent to 1.5×10^{-8} watts of dissipation in the crystal. It is interesting to note that the aging rate is reduced to about 4×10^{-9} per day after about 12 hours and to 2×10^{-9} per day after 20 hours. This rate of stabilization is significantly faster than has previously been observed with other crystal types, and may represent improvements in assembly processes.[1]

(d) PRELIMINARY RETRACE MEASUREMENT. A preliminary retrace measurement was made using the test oscillator configuration with essentially no reactive tuning elements. Crystal #161 was exposed to three cycles of cold soak at -40°C for 16 hours, followed by

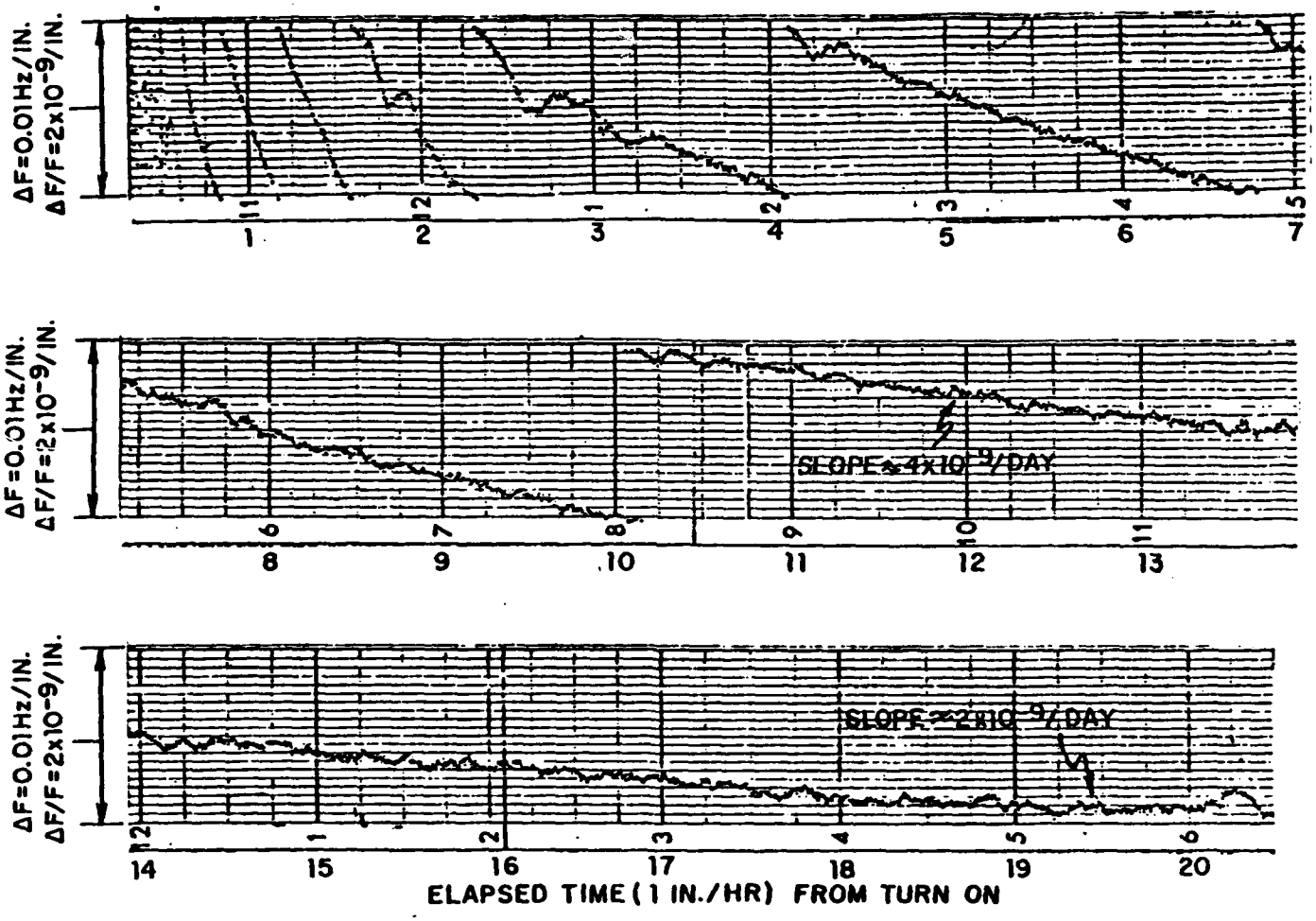

FIGURE 4-9 - FREQUENCY VS. TIME FOR CRYSTAL #157

operation for 8 hours. The variation of the stabilized frequencies for the three cycles are shown in Table 4-1.

TABLE 4-1. RETRACE CRYSTAL #161

CYCLE NO.	STABILIZED FREQUENCY	Δ F FROM 1ST CYCLE	Δ F/F FROM 1ST CYCLE
1	5,114,961.29193 Hz	-	-
2	5,114,961.28110 Hz	-.01083 Hz	-2.1×10^{-9}
3	5,114,961.28808 Hz	-.00385 Hz	-0.5×10^{-9}

(e) SHORT-TERM STABILITY MEASUREMENTS. Evaluation of the developmental ceramic package crystals for short-term stability has been a continuing effort, with some degree of inconsistent results. Chronologically, the measurements were made as follows.

During January 1979, crystals were operated at various levels of current in a limiting type of oscillator circuit shown in Figure 4-10. The result of short-term stability measurement on these units is shown in Figure 4-11. The Δ F/F for crystals 90, 157, and 161 are shown for various crystal currents. The results are similar for each crystal, differing at most by a factor of two for comparable currents and measurement time. As expected, the stability improves with increasing crystal current. However, the curves seem to suggest that other factors start to dominate for measurement time greater than ten seconds.

Crystal 161 was also operated in the test oscillator circuit shown in Figure 4-6 which uses AGC and is without reactive components. These results are shown in Figure 4-12. For measurement times greater than ten seconds, the Allan variances were computed from ten second data by averaging blocks of readings.

In an effort to determine if the test oscillator was causing significant contribution to the stability data, the stability of the fundamental crystal installed in the FTS B5400 oscillator, manufactured by Frequency and Time Systems, Inc., Danvers,

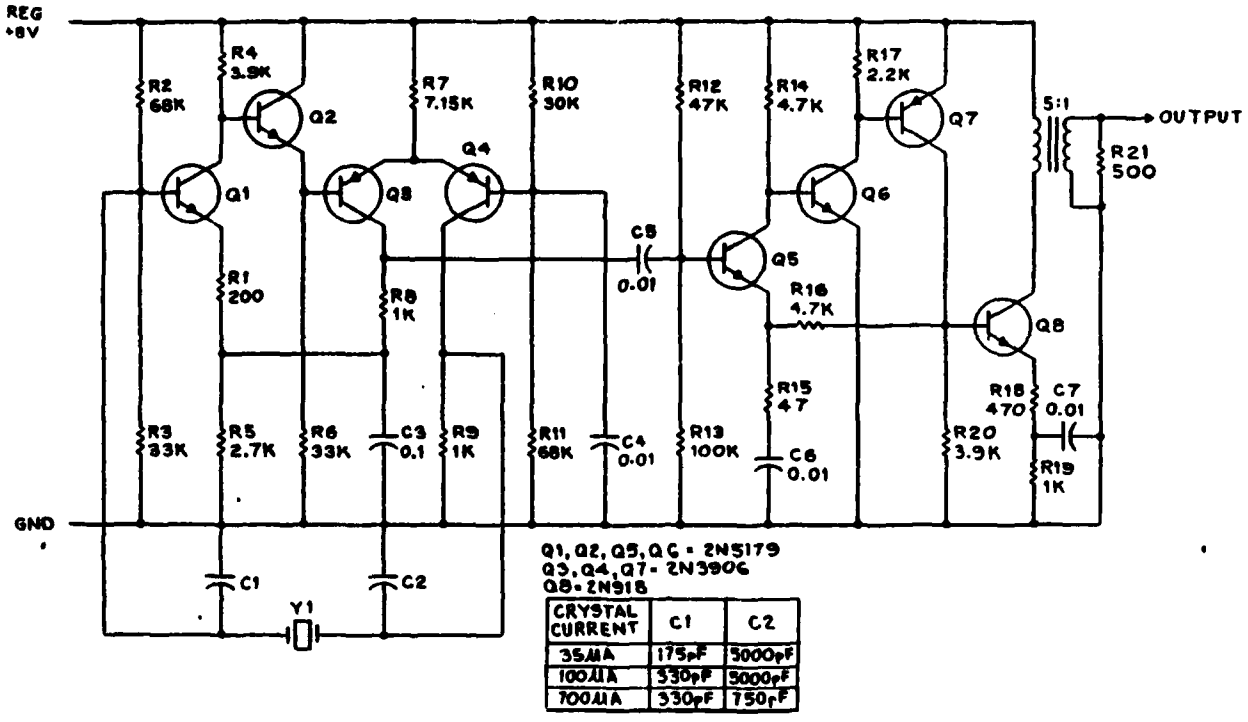

CRYSTAL CURRENT	C1	C2
35MA	175pF	5000pF
100MA	330pF	5000pF
700MA	330pF	750pF

FIGURE 4-10 - SELF LIMITING OSCILLATOR CIRCUIT

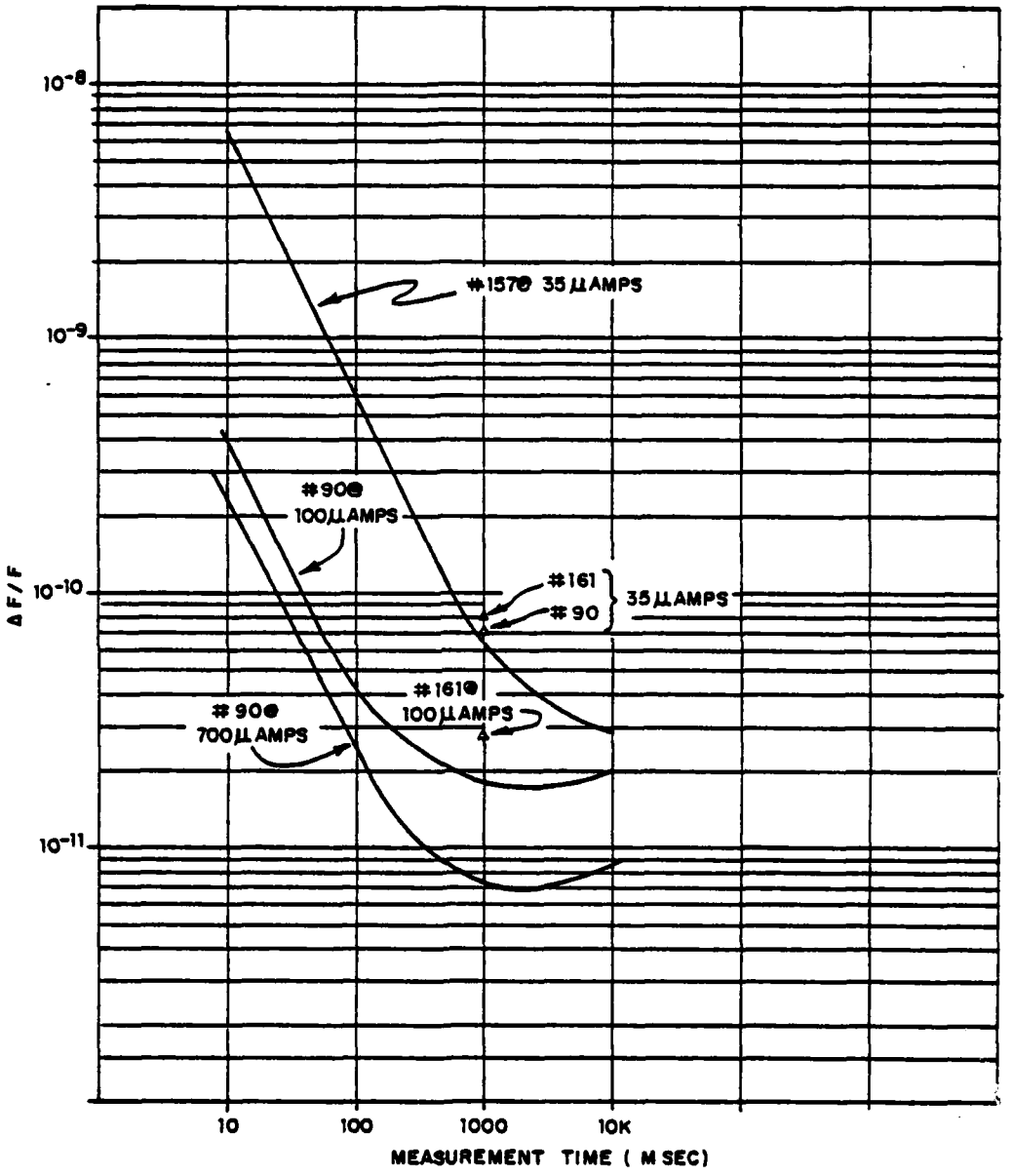

FIGURE 4-11. SHORT TERM STABILITY MEASUREMENTS

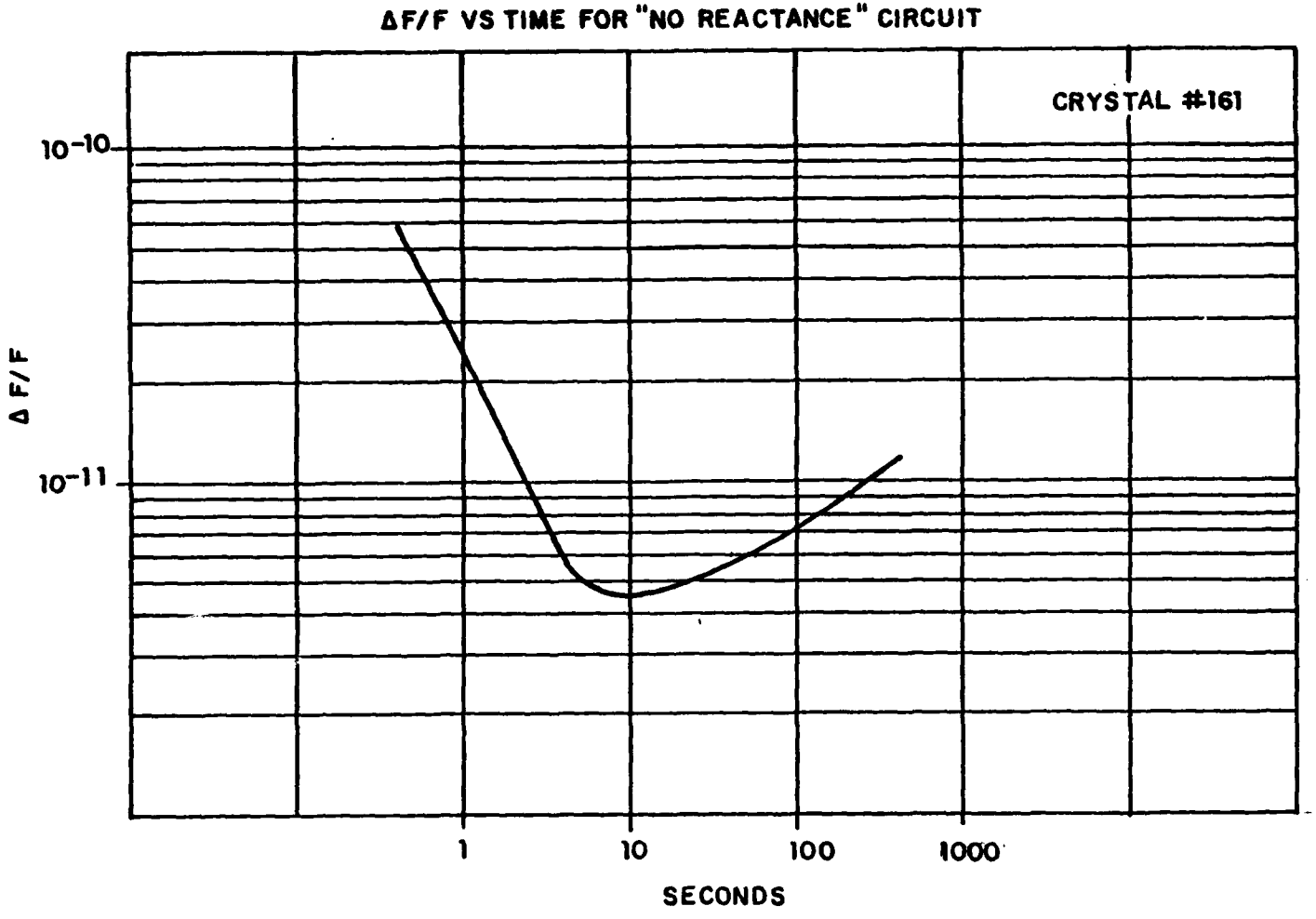

FIGURE 4-12

ΔF/F VS TIME FOR "NO REACTANCE"
CIRCUIT (CRYSTAL #161)

Massachusetts, was measured to provide a comparison with data from our own test oscillators. The FTS oscillator provides 1×10^{-12} $\Delta F/F$ (1 second) with a fifth overtone crystal. Crystal #90 was installed with only slight modification to the oscillator to maintain crystal current at about the original value of 300 microamps, and to accommodate the higher turn temperature of the fundamental crystal. Figure 4-13 shows the Allen variance obtained with the fundamental crystal in this oscillator, indicating performance comparable to that obtained in our test oscillators.

In addition, a crystal was operated in the circuit described in paragraph 4.2.1.2. Initial stability performance measurements indicate $\Delta F/F$ (1 second $< 1 \times 10^{-11}$). Figure 4-14a shows initial data with crystal #161 on 19 March 1979. This stability trace is representative of all oscillators tested using the fundamental crystals, with $\Delta F/F$ for longer measurement intervals increasing over 1×10^{-11}. On 22 March, the record (Figure 4-14b) shows a degradation of performance, the cause has not yet been determined. A third overtone 5.6 MHz crystal installed in this oscillator performed as shown in Figure 4-14c.

The third overtone crystal, having considerably smaller motional capacity, may be considered to be less responsive to circuit perturbations. The present effort with the phase perturbation test facility is directed toward resolving the source of these disturbances between the circuit and the crystal itself.

Finally, crystal #161 was installed in one of the original self-limiting oscillators, similar to that described in paragraph 2.1.2.1, with somewhat better short-term stability performance, as indicated in Figure 4-15.

As a result of these measurements, it appears that additional effort is necessary to reduce circuit contribution to the instability of the oscillator. There also appears to be indications of anomalous behavior of these initial developmental crystal units, which necessitate further evaluation.

(3) COMPONENT EVALUATION. In conjunction with the short-term stability evaluation of crystals, work has proceeded in identifying possible sources of perturbations introduced into the oscillator circuit from other components.

FTS B5400 OSCILLATOR WITH FUND. CRYSTAL #90

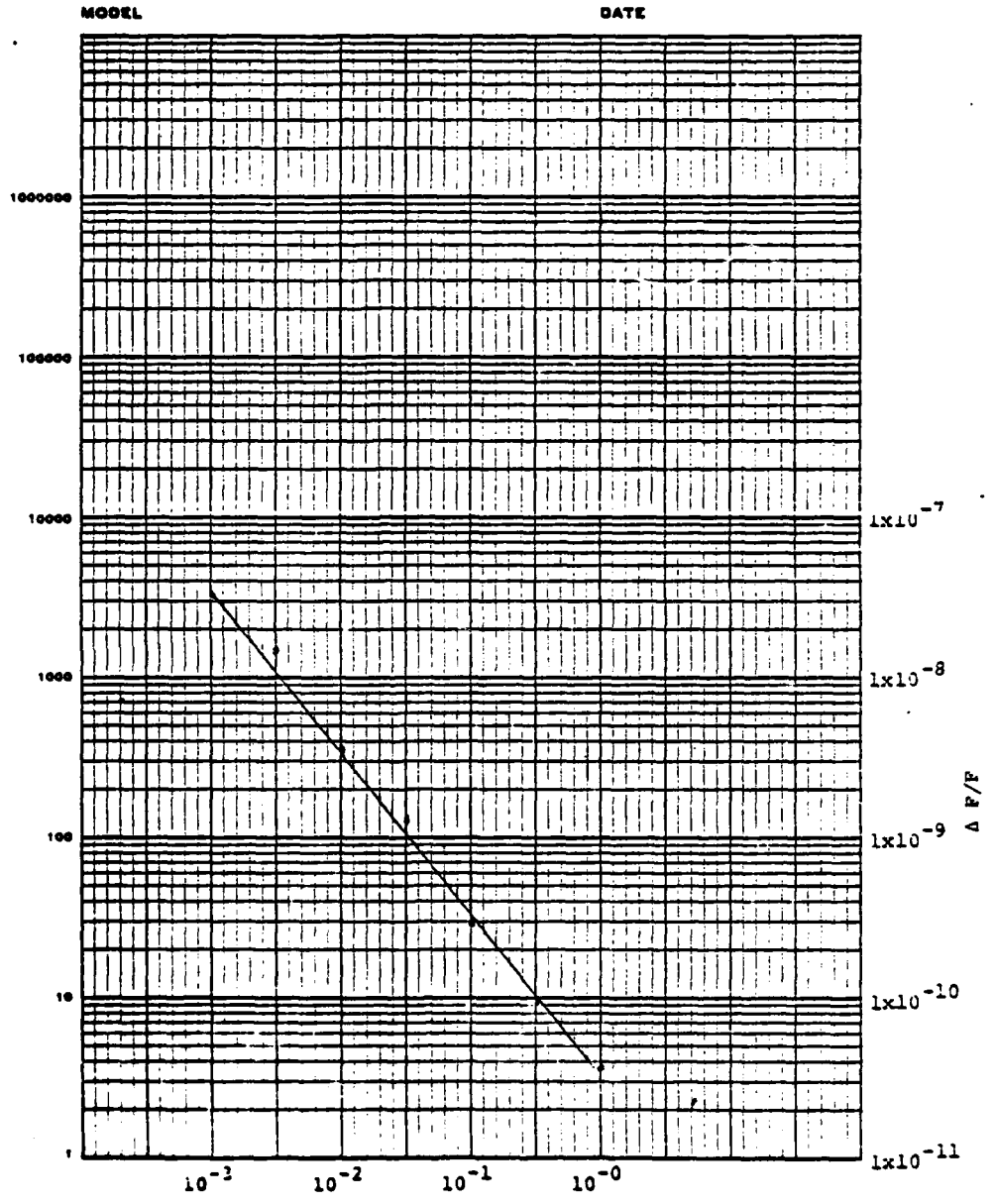

FIGURE 4-13. MEASUREMENT TIME (SECONDS)

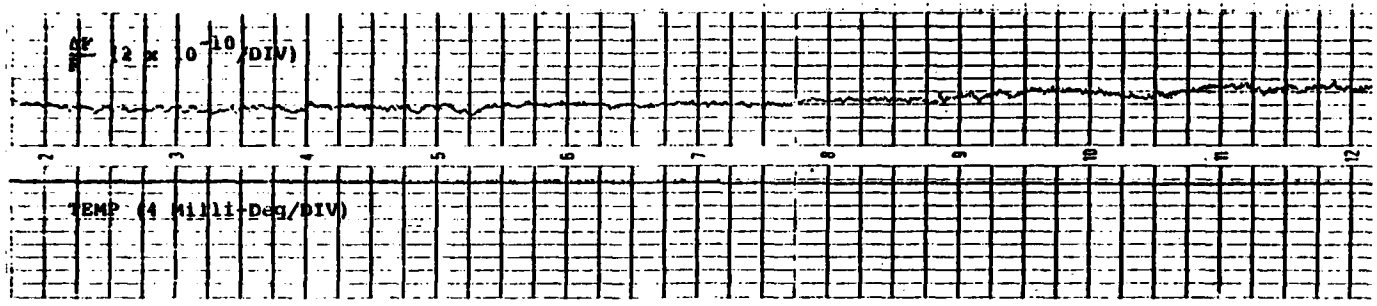

Crystal #161 19 March 1979 FIG. 4-14a TIME (1 IN/HR)

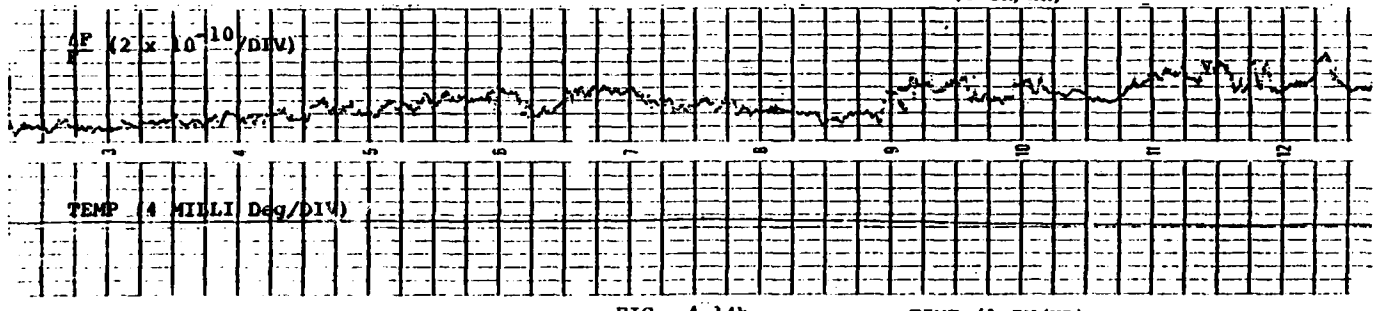

Crystal #161 22 March 1979 FIG. 4-14b TIME (1 IN/HR)

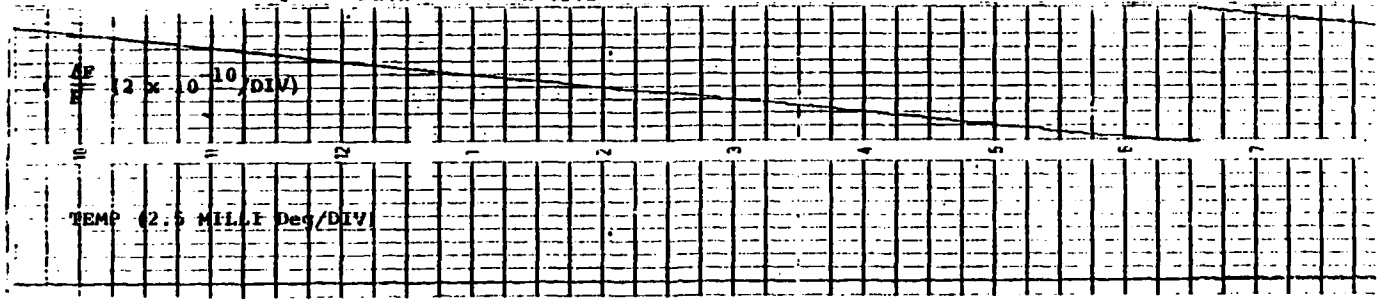

THIRD OVERTONE CRYSTAL FIG. 4-14c TIME (1 IN/HR)

FIGURE 4-14. STABILITY MEASUREMENTS 10 SEC MEASUREMENT TIME INTERVAL

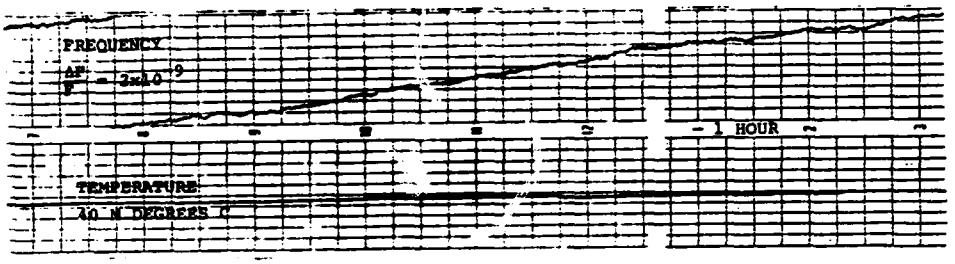

TIME

FIGURE 4-15 - CRYSTAL #161 SELF LIMITING CIRCUIT STABILITY MEASUREMENTS

(a) FLICKER NOISE IN OPERATIONAL AMPLIFIERS. The voltage regulator and temperature control circuits employ a low current, programmable operational amplifier, type 776. These amplifiers may contribute to oscillator frequency instability directly through the introduction of low frequency "flicker" noise to the oscillator from the voltage regulator, and indirectly via temperature variations due to noise in the temperature controller. The noise amplitude has been found to vary considerably among individual units of an amplifier type.

Three candidate amplifier types were evaluated by measuring the noise level of a dozen samples of each type in a standard test circuit providing a gain of 100 x and a source impedance of 1 k ohms.

The types investigated were:

Fairchild	A776HM
Motorola	1776G
RCA	CA3078AT

Within the bandwidth from DC to 1 Hz, units were found to vary from >5 V p/p (referred to the input) to <0.2 V p/p. A level of 1 V p/p is considered acceptable for our application. While all of the RCA units tested were acceptable, several of the other units had excessive noise. It appears that some selection process will be required to ensure acceptable performance for the oscillator application.

(b) MEASUREMENT OF FLICKER NOISE CURRENTS IN TRANSISTORS. Variations of magnitude of the flicker noise component of the collector current of various transistors were investigated. Flicker noise is recognized as a potential source of low frequency phase perturbations of the oscillator, although the severity of the dependence is still under study, as described in the following section.

Small quantities of discrete devices of several types were operated in a test circuit and the magnitude of flicker components from DC to 6 Hz were recorded and are shown in Table 4-2.

It is our intention to procure chip samples randomly selected from several wafers, install these on substrates using processes generated for TMXO assembly, and measure noise performance; then select quantities for use in the program from the wafer having the best performance statistics. Conversations with suppliers indicate confidence that performance correlation among chips from the same wafer is good even for flicker noise.

TABLE 4-2. FLICKER NOISE CURRENT VARIATION

TYPE	MANUFACTURER	RESULT
2N3904	MOTOROLA	1 na P/P to 100 na P/P @ 1 ma Dc
2N3904	ITT	20 na P/P to 200 na P/P @ 1 ma Dc
2N5179	RCA	10 na P/P to 100 na P/P @ 1 ma Dc
2N3906	ITT	1 na P/P to 10 na P/P @ 0.5 ma DC
2N3906	MOTOROLA	20 na P/P to 80 na P/P @ 0.5 ma Dc

4C MECHANICAL DESIGN. Accomplishments in the mechanical design area followed an orderly progression based on optimization of materials, sealing techniques, thermal characteristics, electronic design and production fabrication techniques. These accomplishments and milestone decisions are described in the following subsections.

(1) MATERIALS. Materials selected for use in the TMXO must satisfy a number of highly important and, in some cases, critical requirements. Of primary concern, in all the characteristics of materials to be used in the TMXO, are vacuum performance, (outgassing) and thermal behavior.

A major problem experienced in previous designs of the TMXO (under seperate contracts) has been excessive power aging due to the inability to maintain a vacuum below 1×10^{-4} Torr. It is believed that this lack of performance was caused by outgassing of materials. Another possible cause of loss of vacuum integrity in the baseline design is leakage of the crystal package since it is at a higher pressure than that of the TMXO. Additionally, joining of the two microcircuit packages presents a challenging problem since solders are inherently poor performers in vacuum due to their low vapor pressure.

Of equal importance is the Vespel pedestal used in previous TMXO's. Vespel is a polyimide plastic that exhibits high thermal resistance. However, based on tests by Varian[2] polyimide performs poorly in ultra-high vacuum systems and, after preconditioning by heating and vacuum treatment, absorbs moisture rapidly. These characteristics lead to the conclusion that plastic materials should be eliminated from the TMXO Baseline design and a substitute, with equal thermal and structural properties investigated. Possible candidates for these functional requirements are "super insulation" type materials.

(a) INVESTIGATION OF PEDESTAL MATERIALS. Insulation data received has been reviewed for possible application in the TMXO. Both materials are super insulation types. One is manufactured by Johns-Mansville, called Min-K, and the other is made in England by Micropore Insulation Ltd., called Microtherm. Thermal conductivities of both products compared to that of Vespel which had been proposed for the pedestal are as follows:

	Min-K	Microtherm	Vespel
Thermal Conductivity BTU IN $(FT^2HR\ ^oF)^{-1}$ at 14.7 psia	.21 at 300 ^oF	.21 at 350 ^oF	2.6 at 104 ^oF

Since both insulations are basically microporous structures, their thermal conductivities are reduced significantly in low pressure (vacuum) applications as follows:

	Min-K	Microtherm	Vespel
Thermal Conductivity BTU IN $(FT^2HR\ ^oF)^{-1}$ at reduced pressure	.09 at 350°F (1 Torr)	.055 at 100°C (high vacuum)	2.6 at 104°F

Although thermal conductivities of these super insulations are approximately 25 times lower than that of Vespel, they are not primarily structural materials. Two of the Min-K configurations (TE 1200 and TE 1800) are designated as "Non-Load Bearing" and the maximum compressibility of Min-K (1301) is 8% at 190 psi. The maximum compressibility value of Microtherm is 5% at 3K gcm^{-2} (42.6 psi).

For structural comparison with Vespel, which has a compressive modulus of 569×10^3 psi at 73°F, a compressiblity of 8% at 190 psi yields a compressive modulus of $E = 190/.08 = 2.4 \times 10^3$ psi, which means that a Min-K pedestal configured in the form of the proposed Vespel pedestal would be 25 times more thermally isolative, but would be 569/2.4 = 237 times less rigid, and would be structurally inadequate. The above comparison, made using the compressive modulus, should also consider the flexural and tensile moduli for worst case consideration but Min-K and Microtherm data is not available for flexure and tension.

The Vespel pedestal application technique must be modified for the non-structural Min-K or Microtherm materials if advantage of their thermal superiority is to be gained. For comparison purposes, the configuration shown on the next page has been proportioned to provide equal thermal transfer with the Vespel pedestal. Some modification of this configuration may be a practical application dependent upon the strength, but complete strength data is not available at present.

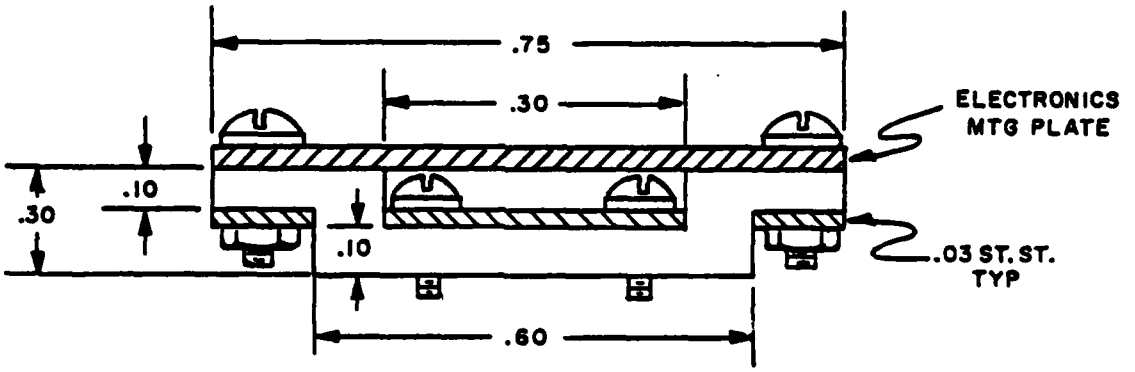

Estimate of Supported Weight - Lbs.

Estimated Crystal Assembly	.0051 (3.3 gms)
Estimated Electronics Assembly	.0110 (5 gms)
Electronics Mtg. Plate .75 x .75 x .032 x .32	.0058
Center Plate $\frac{\Pi \times .3^2}{4}$ x .032 x .29	.0007
Ring Plate $\frac{\Pi(.75^2 - .6^2)}{4}$ x .032 x .29	.0015
Insulation $.75^2$ x .3 x .03	.0022
	.0263
Miscellaneous	x 1.5
	.039 Lbs.

Thermal Transfer Factor A (K_T/L)

K_T = Thermal Conductivity $\frac{\text{BTU in.}}{\text{HR Ft}^2\ ^\circ\text{F}}$

A = Area (in^2)

	Vespel	Insulation
$A(\frac{K_T}{L})$ =	$\frac{\pi(.47^2 - .445^2)}{4} (\frac{2.6}{.48})$	$\frac{\pi(.6)^2}{4} (\frac{.1}{.3})$
	= .097	= .094

The configuration shown will have nearly identical thermal transfer with the proposed Vespel pedestal and when compared with the compressive data available, will have somewhat less compressive rigidity.

Spring Rate $K_s = AE/L$ for Compression

(For Least Rigid Section)

	Vespel	Insulation
K_s =	$\frac{.018(569 \times 10^3)}{.37}$	$\frac{.212\ (2.4 \times 10^3)}{.1}$
K_s =	2.77×10^4	5.09×10^3

Natural Frequency $f_n = \frac{1}{2\pi} (\frac{K_s g}{W})^{1/2}$

	Vespel	Insulation
f_n =	$\frac{1}{2\pi} (\frac{2.77 \times 10^4 \times 386}{.039})^{1/2}$	$\frac{1}{2\pi} (\frac{5.09 \times 10^3 \times 386}{.039})^{1/2}$
f_n =	2.64×10^3	1.13×10^3

A natural frequency of 1.13×10^3 would result in a pedestal resonance below 2000 Hz. Since the design goal is 2000 Hz, pedestal configurations should be proportioned to have natural frequencies of at least $2000/.7 \cong 2800$ Hz to avoid vibrational amplification greater than 2. It is important to note that the lowest Vespel pedestal natural frequency is in the flexure mode and is also below 2800 Hz. Since the original vibration requirement was at 500 Hz maximum, the proposed pedestal was configured for that requirement. The flexure natural frequency for the Vespel pedestal as a cantilever beam is determined as follows:

$$f_n = \frac{1}{2\Pi} \left(\frac{K_s g}{W}\right)^{1/2}$$

K_s = Spring Rate = $\frac{3EI}{L^3}$ for cantilever beam

E = Flexural Modulus = 440×10^3

I = Area Moment of Inertia = $\frac{\Pi(d_o^4 - d_i^4)}{64} = 4.7 \times 10^{-4}$ IN^4

L = Beam Length (Thin wall section only) - .37 IN

$$K_s = \frac{3(440 \times 10^3)(4.7 \times 10^{-4})}{.37^3} = 1.22 \times 10^4$$

g = Gravitational Acceleration = 386 in/sec^2

W = Total Weight - .039 Lbs.

$$f_n = \frac{1}{2\Pi} \left(\frac{1.22 \times 10^4 \times 386}{.039}\right)^{1/2} = 1.75 \times 10^3$$

Some sacrifice of thermal isolation may be necessary to increase the Vespel pedestal natural frequency to 2800 Hz by either making the pedestal shorter or increasing the wall thickness.

For the insulative pedestal, maximum stress will occur at the .3 inch dia. circumference and will result from side loading. Assuming a 1G side load:

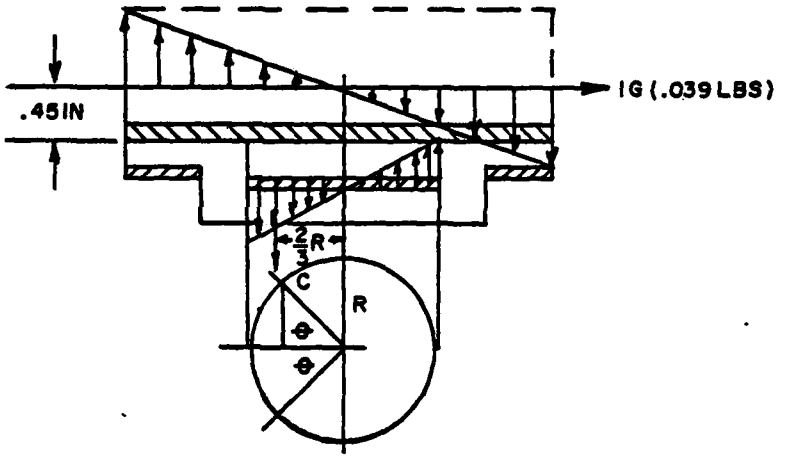

Combined load can be considered to react at 2/3R which means the bulk of load is resisted along a 2θ arc.

Stress Distribution:

θ = Arc cos 2/3 = 48.2

2θ = 96.4°

Stress Length = $\frac{96.4}{360}$ Π (.30) = .252 IN

Stress Area = .252 IN (.10 THK) = .025 IN^2

M = 1G (.039 LBS)(.45 IN) = .0176 IN LBS Overturning Moment

C = Restraining Load = $\frac{M}{2/3R} = \frac{.0176}{2/3(.15)}$ = .176 LBS

$$\text{Stress} = \frac{C}{\text{Stress Area}} = \frac{.176}{.025} = 7.04 \text{ psi}$$

Min-K data sheet gives the average transverse strength (assumed to be shear) as 55 psi for 1301 which indicates adequate strength for a 55/7.04 = 7.8 G load. This is probably not adequate for a tactical environment.

This preliminary investigation indicates that the superior thermal characteristics of Min-K and Microtherm are more than offset by the poor load carrying capability of the non-structural materials. However, more thermal and structural data as well as sample materials have been requested from Johns-Mansville and Micropore for continued investigation and tests.

Materials, known to be low in outgassing and capable of being preconditioned at high temperatures were investigated. Amongst these were glass[3], ceramic and glass bonded mica. Comparisons of the thermal properties of these materials to Vespel prevented them from being further considered due to the extremely thin wall that would be necessary to match the thermal losses in the Vespel pedestal.

(b) MICROCIRCUIT PACKAGE. Drawings of the microcircuit package shown in Figure 2-7 were sent to approximately 20 suppliers of similar products. Due to the material required (Beryllia), and the anticipated problems with providing feed thrus with very low leak rates, only one supplier responded. Alternate materials were considered, but due to the need to approach an isothermal environment around the crystal, utilizing a single heat source (the heating transistor), the effort was abandoned.

(c) WIRES. In considering the requirements on the wires providing power and signal interfaces to the microcircuit package, several characteristics become primary for consideration. Amongst these are thermal conductivity, electrical resistivity and modulus of elasticity. Additionally, expansion coefficient could become important based on the method finally selected for sealing the wires as they egress the package. Table 4-1 shows the candidate wires and their properties. The TMXO requires five wires for external connection. Two wires are used for power (up

to 10 watts at 12 volts) and three are used for signals (no significant power). The current requirement for the power wires is:

For the power wires:

$E = 12V$

$P = I^2R$

$E = IR$

By substitution,

$$R = \frac{E^2}{10} = \frac{(12)^2}{10} = 14.4 \text{ ohms}$$

Therefore,

$$I = \frac{E}{R} = \frac{12}{14.4} = .833 \text{ amps}$$

Using the following equations, a comparison, based on one wire .010" in diameter and .50 inches long can be made as shown in Table 4-3.

$$A = \frac{(.010)^2\pi}{4} = 7.85\text{x}10^{-5} \text{ in}^2 = 5.45\text{x}10^{-7} \text{ ft}^2 = 5.067\text{x}10^{-4}\text{cm}^2$$

$$L = .5 \text{ in} = 4.167\text{x}10^{-2} \text{ ft} = 1.27 \text{ cm.}$$

$$Q = \frac{KA}{T}\Delta t \qquad \Delta t = 234°F$$

$$P = I^2R \qquad I = .833 \text{ Amps}$$

$$\text{Elect wire Res} = R_1\left(\frac{L}{A}\right) \qquad \frac{L}{A} = \frac{1.27\text{cm}}{5.067\text{x}10^{-4}\ \text{cm}^2} = 2.51\text{x}10^{3}\ \text{cm}^{-1}$$

$$\frac{A}{L}\Delta t = \frac{5.45\text{x}10^{-7}}{4.167\text{x}10^{-2}} \qquad (234) = 3.06\text{x}10^{-3}\ \frac{\text{ft}^2}{\text{ft}}\ °F$$

The data in Table 4-3 will be used in conjunction with other characteristics to determine wire type and size when more firm decisions are made.

TABLE 4-3
WIRE COMPARISONS

Material	Therm. Cond. (BTU) (FT)/ (HR) (SQ. FT) (°F)	Resistivity OHM-cm.x 10^{-6}	Ratio K/R	WIRE LOSSES .010"D.x.5 LONG WIRE Elect. Resist. Ohms	Voltage Drop ΔV	Power Loss ΔWatts W1	Heat Loss Q BTU/HR	Heat Loss Thru Wire Watts Q1
Silver (Pure)	242.0	1.47	164.63	$3.69x10^{-3}$	$3.07x10^{-3}$	$2.56x10^{-3}$	.742	.218
Nickel	49.6	7.48	6.63	$18.8x10^{-3}$	$15.6x10^{-3}$	$13.0x10^{-3}$	.152	.045
Gold	172.0	2.19	78.54	$5.50x10^{-3}$	$4.58x10^{-3}$	3.8x10-3	.527	.155
Tantalum	31.5	12.50	2.52	$31.4x10^{-3}$	$26.2x10^{-3}$	$21.8x10^{-3}$	.097	.028
Palladium	41.0	10.00	4.10	$25.1x10^{-3}$	$20.9x10^{-3}$	$17.4x10^{-3}$	.126	.037
Kovar	10.2	49.00	.21	$123x10^{-3}$	$102x10^{-3}$	$85.3x10^{-4}$	.031	.009
Stainless Steel	9.4	72.00	.13	$180x10^{-3}$	$150x10^{-3}$	$125x10^{-3}$	.029	.0085

(2) SEALING TECHNIQUES. Several manufacturers of welding equipment have been contacted to determine the applicability of their equipment to the sealing of the outer case of the TMXO. It must be noted that the design of the outer case, the material, the header design, and the size of the unit are impacted by the sealing technique selected. A promising welding technique is Ultrasonic welding. The weld is complete in less than one second and generates little heat. Use of this technique would require an aluminum outer case with a .020 inch flange.

An investigation into the methods used by a crystal manufacture in sealing their high quality glass crystal package, was conducted.

The following data was obtained.

1. The glass case is fused to the glass header with induction heating localized to a kovar washer imbedded in the base.
2. The names of the manufacturer of the base and the glass case were obtained.
3. The sealing operation takes about 1 minute.

The base manufacturer was contacted and has provided Bendix with samples and drawings of the Bliley parts. The technique is very promising and led to the generation of a new approach to the packaging design of the TMXO as discussed in paragraph 4.3.4.

Indications are that a similar technique could be used for the outer housing seal. However, a thorough investigation of this seal is continuing.

(3) THERMAL ANALYSIS. Frequency stability of the TMXO over the ambient range of $-54^{o}C$ to $+75^{o}C$ is directly related to temperature stability of the crystal. Due to the extremely low power available (.25 watts) and the varying delta temperature involved in the design,

Highest $t = (94 - (-54)) = 148^{o}C$

Lowest $t = (84 - +75) = 9^{o}C$

A computer program was written to evaluate the overall thermal characteristics of the TMXO. The following is a description of the program.

The program is configured to offer many options to the user such as:

a. Microcircuit package area.
b. Pedestal cross sectional area.
c. Power and signal wire diameter, length and thermal conductivity.
d. Crystal Temp.
e. Internal pressure

To allow some comparative evaluations to be made, certain assumptions and conditions had to be estimated. Additionally, since the radiation losses from the package to the inside walls are non-linear, the decision was made to determine the losses under the following conditions:

a. Vespel pedestal; Cross Sectional Area = 1.248×10^{-4} ft^2, K = 2.4 BTU ft/HR $ft^{2o}F$, L = .48 inches
b. Power wires .010" D. x .5" long with a K of 112.8 BTU ft/HR $ft^{2o}F$. (Stainless Steel) (Quant. 2).
c. Signal wires .003" D. x .5" long, same K (Quant. 3).
d. Circuit Surface Area - 1.389×10^{-2} ft^2.

These values were set into the program to allow the emissivity combination factor FE to be determined. The conditions were that the total dissipation (Q1) should equal .25 watts at -54^oC ambient and with the highest expected crystal temperature of 94^oC in the unit. Values were then plotted for:

Q1 = Total Power
Q2 = Power lost thru the pedestal
Q3 = Power lost thru the power wires
Q4 = Power lost thru the signal wires
Q5 = Power lost thru radiation
Q6 = Power lost thru conduction thru air inside the package.

Figure 4-16 shows the result of this plot.

C1 = Emissivity value needed between the inside surface circuit crystal and the inside of the package. Since the emissivity value of the circuit and crystal package is unknown at this time, a table (Table 4-4) is printed out to allow a determination of the emissivity needed for the inside case surface vs. emissivity

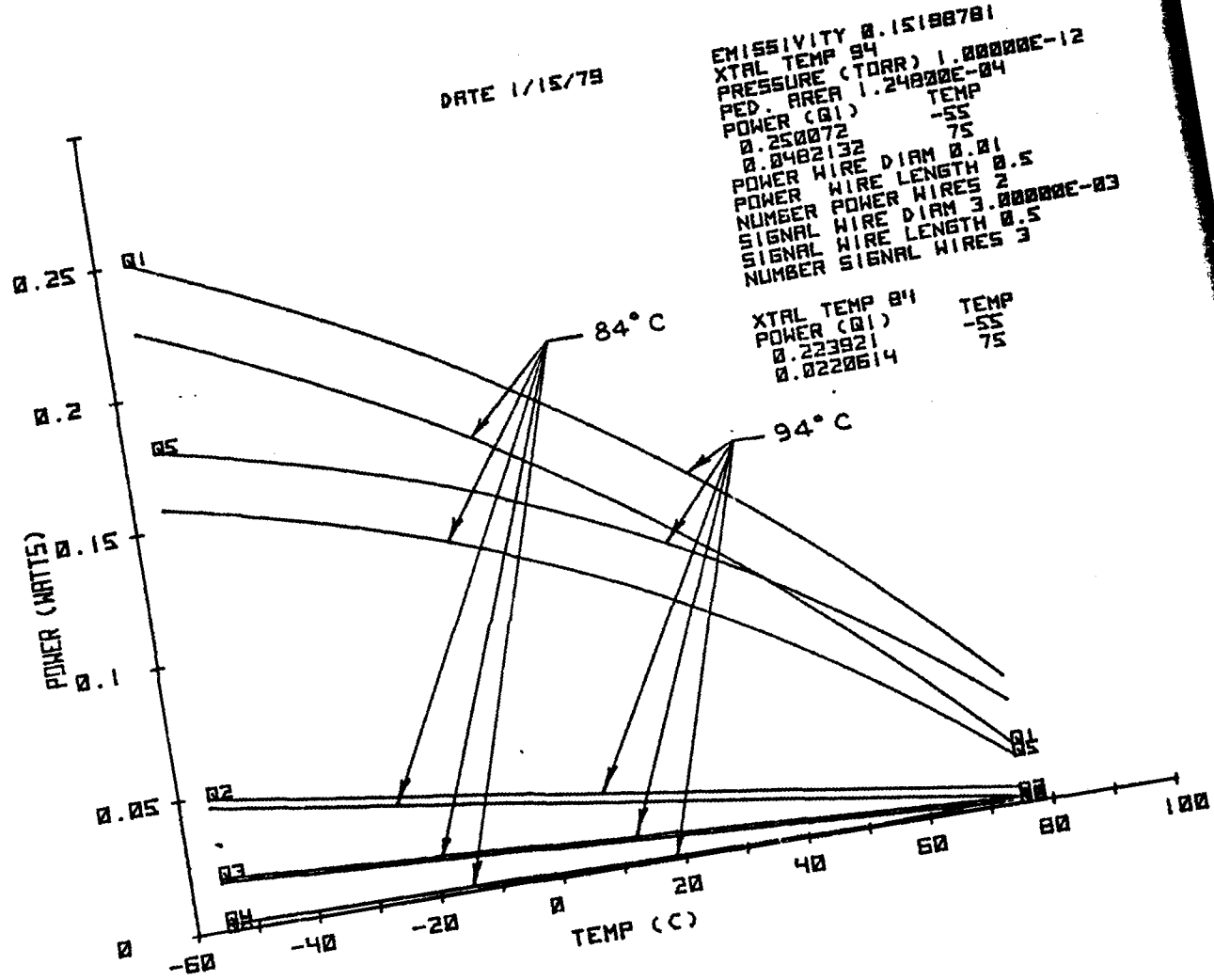

FIGURE 4-16. THERMAL PLOT

of the crystal and circuit package. Therefore, the combination of E2 and E3 shown will result in the desired C1. For example, in Table 4-4; if E2 = 0.7 then E3 must = .10755. This is a reasonable emissivity value for many metals.

This emissivity value (C1) is then set into the program and the plots made as shown in Figure 4-16. Note that the crystal temperature is then changed to 84°C, with all other conditions remaining the same, and a new plot generated to determine the power losses at 75°C ambient with the low temperature crystal installed.

In the cases shown, the losses at 75°C (.02206 watts) are lower than the minimum power needed to operate the oscillator. This condition would result in an out of control situation at the high ambient. To maintain control, the heater should be adding heat under all environments. The minimum oscillator power is expected to be .036 watts.

This clearly shows that meeting the specification requirements at -54°C of .25 watts is obtainable. However, meeting the requirements at 75°C ambient, with the 89°C $\pm$5°C crystal is questionable.

Table 4-5 shows calculations made under various conditions. Plots No. 1 thru 5 show how the high ambient power is affected by the nominal crystal temperature as well as the tolerance. Plots 2 and 3 show the results from designing for .25 watts for the nominal crystal at -54°C. Plots 6-12 show the impact of internal pressure on maximum power at -54°C. In plots 11 and 12, the calculated value of C1 goes below 0. This is then set to .15 and the powers calculated and plotted. Plots 7 and 8 are directly comparable to Plot 3 and indicate the impact of pressure in the TMXO. Plots 7, 10, 11 and 12 can be compared to Plot 4 to determine the impact of rising pressure in the TMXO.

TABLE 4-4. EMISSIVITY TABLE FOR C1 = 0.151987810

E2	E3
1	0.100116882
0.95	0.100974017
0.9	0.101943766
0.85	0.103049886
0.8	0.104323317
0.75	0.105805127
0.7	0.107551019
0.65	0.109638495
0.6	0.112178674
0.55	0.115336727
0.45	0.124698057
0.4	0.132067570
0.35	0.142927835
0.3	0.160528775
0.25	0.193959951
0.2	0.282129219
0.15	1.163416342
0.1	-0.221712889
0.5	-0.048496691

Present plans are to expand the program to include a determination of the impact on crystal temperature with variations in the design and the ambient. Additionally, efforts will continue to determine the proper combination of area and conductivities to allow the temperature extremes to be met. Initially, it appears that raising the nominal crystal temperature would be the best approach.

It must be recognized however, that the program takes a simplified approach to the overall problem in that the results

TABLE 4-5
THERMAL PLOT RESULTS

	1	2	3	4	5	6	7	8	9	10	11	12
Max. Xtal Temp. (°C)	94	94	91	94	102	91	91	91	94	94	94	94
Nominal Xtal Temp. °C	89±5	89±5	89±2	92±2	100±2	89±2	89±2	89±2	89±5	89±5	89±5	89±5
Min. Xtal Temp. °C	84	84	87	90	98	87	87	87	-	-	84	84
C1 (Emissivity)	.15199	.164	.164	.15198	.1349	.1636	.1603	.1266	.1484	.11578	<β Set .1	<β Set .1
Power at -54°C	.25	.264	.256	.250	.250	.2557	.2584	.2551	.250	.250	.5932	2.25
Power at +75°C (Min.)	.022	.023	.0316	.0375	.0537	.032	.0313	.0288	-	-	.045	.139
Pressure (Torr)	-	-	-	-	-	$1x10^{-4}$	$1x10^{-3}$	$1x10^{-2}$	$1x10^{-3}$	$1x10^{-2}$	.1	.5

shown do not consider the actual thermal losses from the crystal to the ambient. Pictorially, the conditions are as shown in Figure 4-17. It is recognized that this approach is less than accurate, but certain conclusions and positive directions can be made and identified in using the program.

The next natural step is to define a more complex thermal loss program that, in addition to allowing calculation of crystal temperature changes with changing ambients, allows the impact on warm-up time to be analyzed based on materials, shapes and configuration. To accomplish this, an effort has commenced to define the thermal parameters of the design in electrical equivalent circuit terms[4,5]. The results will allow a standard circuit analysis program to be used to determine temperature variations expected at the crystal under various conditions. Warm-up time and heater to sensor impacts may also be determined.

An equivalent electrical circuit design of the thermal paths and capacities of the design was generated. The first attempt at this task is shown in Figure 4-18. This RC network will be analyzed in a standard computer program and will be used to predict the various temperatures and warm-up times based on the values assigned to the individual thermal resistive and capacitive elements as the design evolves. Calculation of these assigned values may draw on known solutions to three-dimensional heat flow problems as used by transistor and integrated circuit designers, as well as simpler techniques, where appropriate, for some other components of the system. Efforts have begun to define and accomplish a nodal analysis of the internal parts of the TMXO (inside the glass enclosure). This analysis will be incorporate with the schematic shown in Figure 4-18.

Beryllia has been tentatively selected to act as a heat spreader between the transistor and the crystal. The materials considered were Alumina, Beryllia, Copper and Aluminum. The thermal characteristics are shown in Table 4-6.

Aluminum and BeO are similar in a Thermal Conductivity to weight basis and Aluminum is superior in Heat Capacity. However, BeO was selected to minimize plating and joining problems.

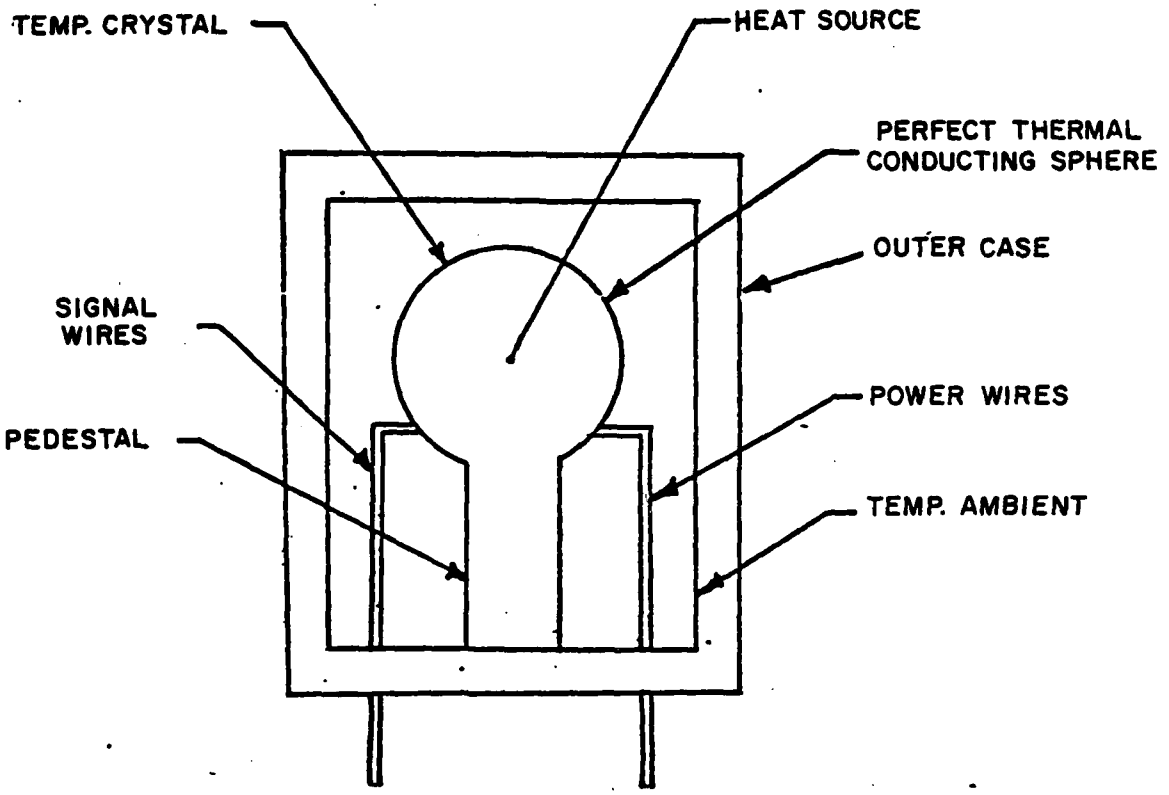

FIGURE 4-17 - MODEL FOR THERMAL PROGRAM

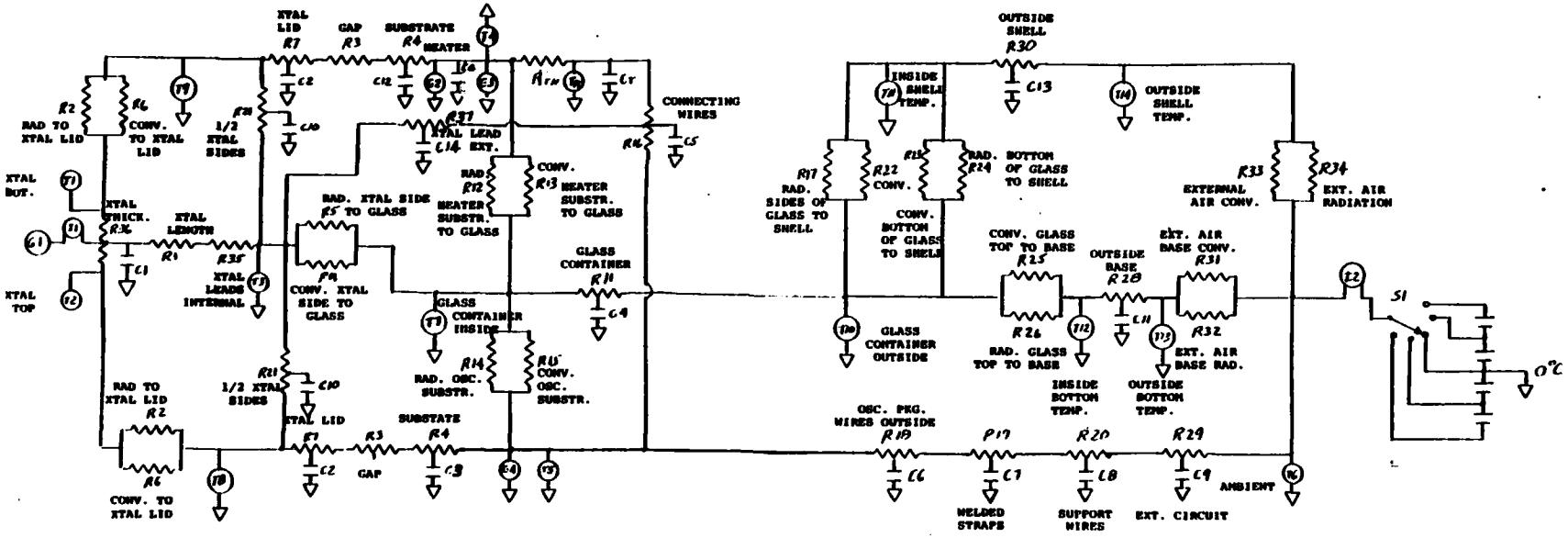

FIGURE 4-18

THERMAL SCHEMATIC

TABLE 4-6

HEAT SPREADER CHARACTERISTICS

	THERMAL CONDUCTIVITY (K) Cal/Sec Cm °C	DENSITY(ϱ) Gm/Cm^3	SPECIFIC HEAT Cal/Cm °C	K/ϱ $Cal\ Cm^2/Cm\ Sec$	Specific Heat xϱ Cal/Cm^3 °C	HEAT CAPACITY $WATT\ Sec/Cm^3$ °C
BeO	.5	2.88	.31	.1736	.8928	3.738
Cu	.94	8.94	.09	.105	.8046	3.369
Alumina	.067	3.90	.223	.0172	.8697	3.641
Aluminum	.479	2.70	.21	.1774	.567	2.374

(4) OVERALL CONFIGURATION. The original concept described in paragraph 2.2.2, was examined and a number of alternate methods of materials, arrangement and techniques examined.

Several major components of the system and the techniques employed to join the components were addressed with primary and secondary considerations in mind. A review of these considerations and their impact is appropriate.

A. Vacuum for Thermal Isolation. The components, assembly techniques, and materials must be compatible with high vacuum and must exhibit a low degree of outgassing in a high vacuum. They must be easily preconditioned prior to assembly to remove the imbedded and surface gas molecules in the material. It must be noted that, due to the critical nature of the crystal and the electronic components, outgassing of some of the components and assemblies is limited to approximately 200°C depending upon the assembly methods used. For example, if solder were used extensively for assembly, a solder schedule could reduce the final breakout below 200°C.

B. Thermal Radiation. As indicated in paragraph 4.3.3, a careful control of the emissivities of the inner component surfaces and the inside wall of the enclosure is necessary. Control of the crystal package, microcircuit package and pedestal surfaces is a high risk area since typically these components have a natural high emissivity. Thus, very low emissivities would have to be obtained for the outer enclosure.

C. Microcircuit Package. The microcircuit package, due to the need to spread the heat to the crystal package, was required to be fabricated from Beryllia. All feed-thrus, joints and joining techniques are required to be leak-proof to prevent contamination by outgassing and pressure rise above 1×10^{-3} TORR. Pressures above 10×10^{-3} TORR cause excessive heat to be lost from the crystal package due to conduction thru the gas.

Microcircuit manufacturers were hesitant to participate in the design shown in Figure 2-7 due to the difficulties anticipated in reliably manufacturing a Beryllia package with feed-thrus and joints with the leak rates specified.

D. Joining Techniques. Joining of the packages resulted in the use of materials known for their poor performance in a vacuum concerning outgassing[6].

E. Pedestal Material. The pedestal must be structurally sound and result in a low thermal path to the base of the package. Additionally, attachment to the base must be structurally sound and not subject to rocking motion in vibration and shock.

As discussed in paragraph 4.3.1.1, no suitable substitute was found to satisfy these requirements.

As a result, a new overall concept was generated and is very promising for a number of reasons. This concept is shown in Figure 4-19. The following advantages are a few of those seen in this approach:

1. The vespel pedestal is eliminated.
2. the μ-circuit packages are eliminated.
3. The design can be reduced to two seals. One for the oscillator package, and one for the outer package.
4. A Dewar type construction is realized since the radiation losses can be controlled with metalization of the glass container and an evacuated container within an evacuated container can be realized.
   Note: Backfilling of the oscillation package is possible and will be decided based on thermal analysis.
5. A cleaner thermal vacuum can be obtained and maintained utilizing materials and techniques proven in vacuum systems.
6. Any contaminations such as epoxies, solder, outgassing etc., will be contained in ther inner chamber and will not affect the thermal vacuum.
7. The thermal paths to the outside environment are minimized.
8. The manufacturing costs are reduced in both purchased parts and assembly labor.
9. Proven techniques are used.
10. The mica support provides alignment during assembly, but most importantly, it adds tremendous support in a shock and vibration environment.

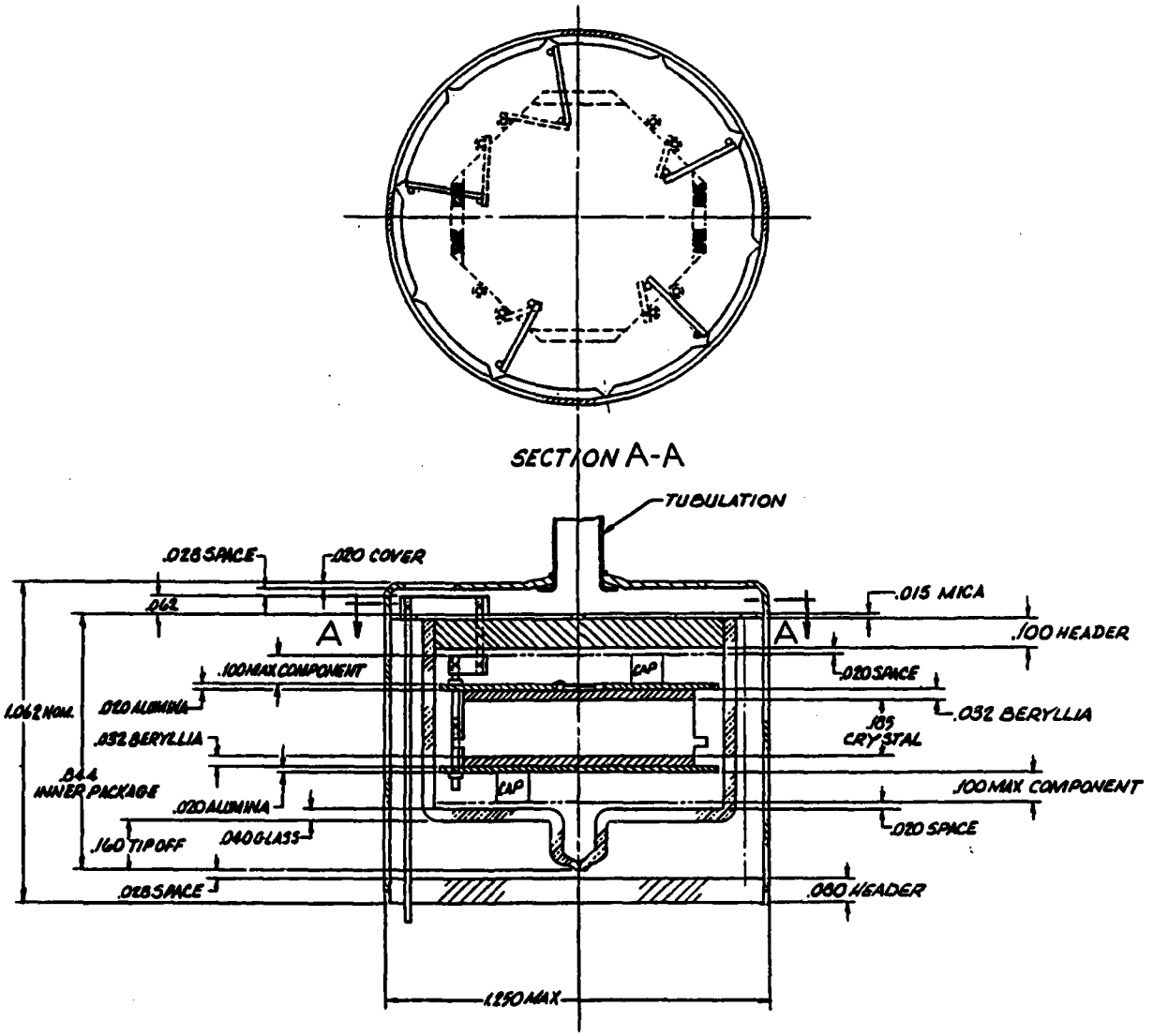

FIGURE 4-19. NEW OVERALL CONCEPT

11. All electrical connections, external and internal are either welded or thermo-compression bonded.
12. Testing can be accomplished at several levels.
13. Ease of manufacturing.

(a) STRUCTURAL CONSIDERATIONS. Elimination of the pedestal obviously requires that consideration be given to the structural integrity of the support system. Additionally, since the support system shown in Figure 4-19 utilizes the five wires needed to operate the TMX0, an optimization of thermal, electrical and structural considerations becomes more straightforward.

Prior to the addition of the mica support, a computer program was written to consider:

1. Thermal losses as a function of diameter and length of the wires.
2. Natural frequency in vibration as a function of diameter and length of wires. The program iterated to allow the two characteristics to be calculated with varying diameters at various lengths. Kovar wires were selected due to their high strength, faily low thermal conductivity, fairly high electrical conductivity and above all its thermal expansion match with glass. The results were promising and show that a length of .8" and a wire diameter of .020 to .025 would be appropriate. Since the moment of inertia, and thus the natural frequency of the system, is a function of the spacing of the wires from the center, a 1" diameter was selected.

TABLE 4-7. SUPPORT STRUCTURE OF 5 KOVAR WIRES

WIRE DIAMETER	NATURAL RESONNANT FREQUENCY	POWER LOSS @ -54°C AMBIENT
0.020 in.	2433 Hz	126 mW
0.025 in.	3042 Hz	197 mW

The diameter, length and material conductivity was then used in the thermal program previously described with the results shown in Figures 4-20 and 4-21. Note that the crystal temperature used, i.e. $89^{o}C + 5^{o}C$, still indicates a lack of control condition at the high ambient with a crystal at the lower turn point temperature.

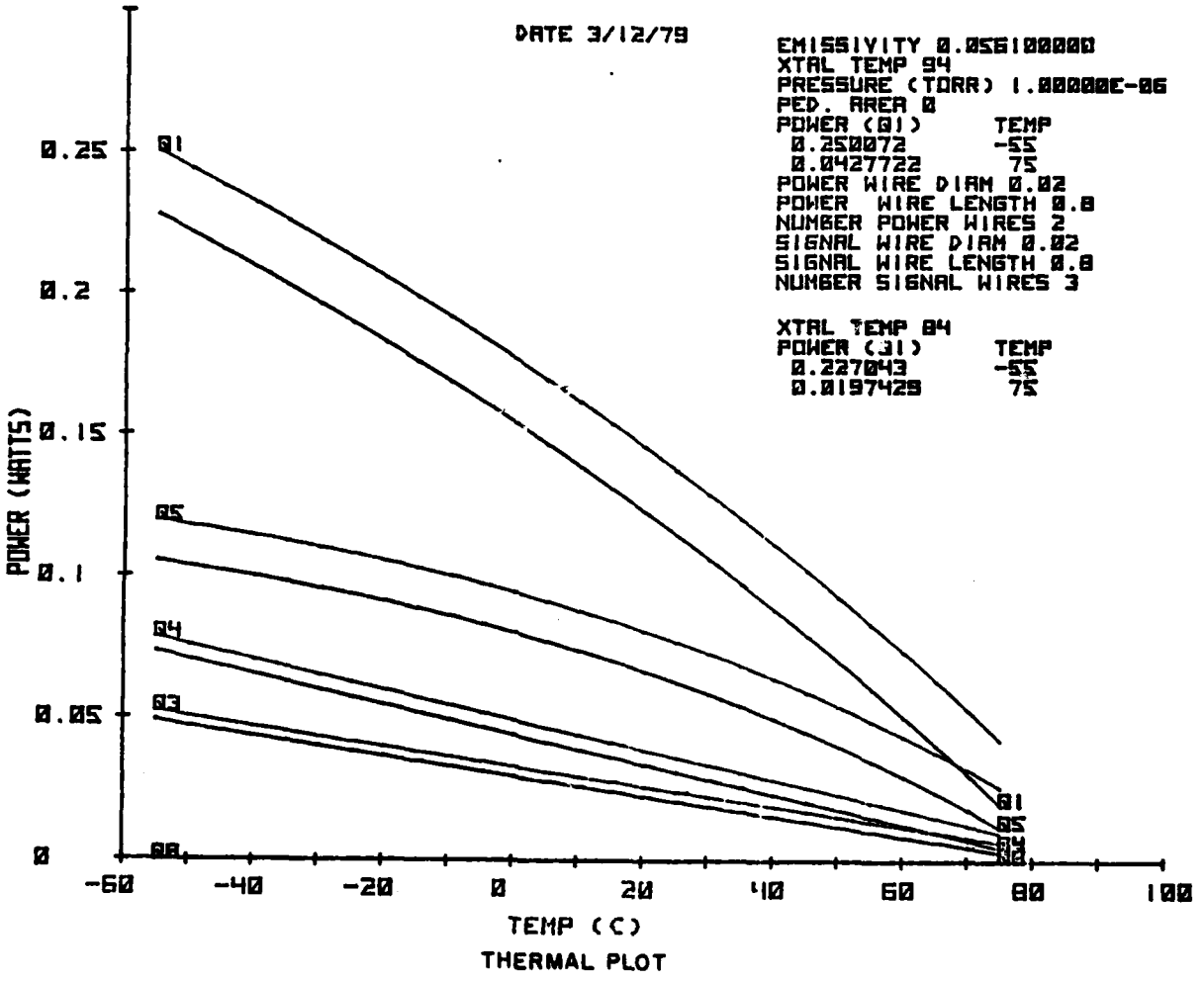

FIGURE 4-20. THERMAL PLOT

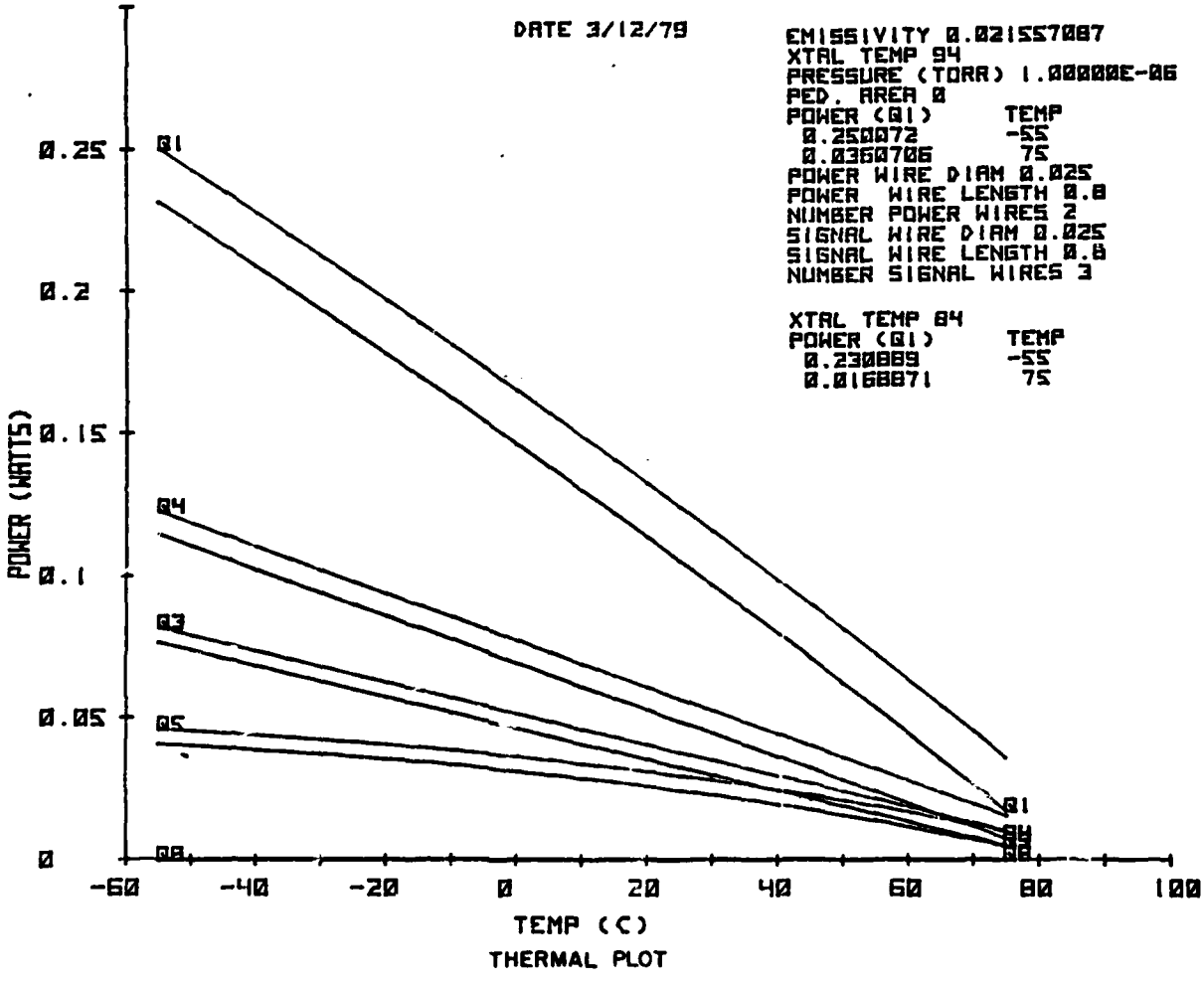

FIGURE 4-21. THERMAL PLOT

5. CONCLUSIONS

As a result of the work performed during this period, we conclude:

(1) The aging and retrace performance of the one crystal tested is satisfactory.

(2) The short-term stability performance of the oscillator/crystal currently falls short of the 1×10^{-11} requirement and has required considerably more investigation than anticipated. This in large part has been due to the need for characterizing the early developmental ceramic flatpack crystal units made available for this program.

(3) A selection process will be required for several of the semiconductor components which can be performed by sampling.

Progress has been made in the area of materials, sealing techniques and thermal analysis. Various techniques and configurations have been investigated with the resultant of a change in the original base line and techniques approach. Materials suspected of being risky in the vacuum equipment have been designed out of the system with a simpler, less risky, producible approach resulting.

6. FUTURE PLANS

Plans for the next six-month period include further evaluation of components and circuits, design and layout of the circuits and mechanical parts, and continued thermal analysis. Efforts will also be expended on material selections and sealing techniques.

REFERENCES

1. R.J. Byrne and J. L. Hokanson "Effect of High-Temperature Processing on the Aging Behavior of Precision 5 MHz Quartz Crystal Units" IEEE Transactions on Instrumentation and Measurement, Vol. IM-17, No. 1, March 1968.
2. P.W. Hait, "The Application of Polyimide to Ultra-High Vacuum Seals". Report VR-42, Varian Vacuum Division, 1966
3. V.O. Altemose and A. R. Kacyon, "Vacuum Compatibility of Machinable Glass Ceramics". Corning Glass Works Report, Corning, N.Y.
4. John P. Buchanan, "Handbook of Piezoelectric Crystals for Radio Equipment Designers". Section IV, Crystal Ovens, WADC Technical Report 56-156, Oct. 1956.
5. Allan D. Drans "Cooling Electronic Equipment", Prentice-Hall, Inc., 1965, P. 104.
6. Yale Stransser, "Review of Outgassing Results", Varian Associates, Vacuum Division, Palo Alto, Calif., Report # VR-51.

MANDATORY CONTRACT DISTRIBUTION LIST

101 Defense Technical Information Center
ATTN: DTIC-TCA
Cameron Station (Bldg 5)
012 Alexandria, VA 22314

203 GIDEP Engineering & Support Dept.
TE Section
PO Box 398
001 Norco, CA 91760

205 Director
Naval Research Laboratory
ATTN: CODE 2627
001 Washington, DC 20375

301 Rome Air Development Center
ATTN: Documents Library (TILD)
001 Griffiss AFB, NY 13441

437 Deputy for Science & Technology
Office, Asst. Sec Army (R&D)
001 Washington, DC 20310

438 HQDA (DAMA-ARZ-D/Dr. F. D. Verderame)
001 Washington, DC 20310

482 Director
US Army Materiel Systems Analysis Actv.
ATTN: DRXSY-T
001 Aberdeen Proving Ground, MD 21005

563 Commander, DARCOM
ATTN: DRCDE
5001 Eisenhower Avenue
001 Alexandria, VA 22333

564 Cdr, US Army Signals Warfare Lab
ATTN: DELSW-OS
Vint Hill Farms Station
001 Warrenton, VA 22186

MANDATORY CONTRACT DISTRIBUTION LIST (Continued)

579 Cdr, PM Concept Analysis Centers
ATTN: DRCPM-CAC
Arlington Hall Station
001 Arlington, VA 22212

602 Cdr, Night Vision & Electro-Optics
ERADCOM
ATTN: DELNV-D
001 Fort Belvoir, VA 22060

603 Cdr, Atmospheric Sciences Lab
ERADCOM
ATTN: DELAS-SY-S
001 White Sands Missile Range, NM 88002

607 Cdr, Harry Diamond Laboratories
ATTN: DELHD-CO, TD (In Turn)
2800 Powder Mill Road
001 Adelphi, MD 20783

609 Cdr, ERADCOM
ATTN: DRDEL-CG, CD, CS (In Turn)
2800 Powder Mill Road
001 Adelphi, MD 20783

612 Cdr, ERADCOM
ATTN: DRDEL-CT
2800 Powder Mill Road
001 Adelphi, MD 20783

680 Commander
US Army Electronics R&D Command
000 Fort Monmouth, NJ 07703
1 DELEW-D
1 DELET-DD
1 DELSD-L (Tech Library)
2 DELSD-L-S (STINFO)
4 Originating Office (DELET-MF)
1 DELEW-V (J. KEEN)
1 DELCS-I (D. LONGINOTTI)

MANDATORY CONTRACT DISTRIBUTION LIST (Continued)

681 Commander
US Army Communications R&D Command
000 Fort Monmouth, NJ 07703
1 USMC-LNO
1 DRCO-COM-RN-3 (R. Shitman)
1 DRCPM-GARS-TM (R. Rugarber)
1 DRCPM-SC (P Maresca)
1 DRDCO-COM-RF-2 (T. J. Klein)

Hewlett-Packard Lab
1501 Page Mill Road
Palo Alto, CA 94304
001 ATTN: Dr. Leonard S. Cutler
001 ATTN: Mr. Donald L. Hammond

Bell Telephone Labs, Inc.
Allentown, PA
001 ATTN: Mr. Warren L. Smith

Cincinnati Electronics Corp.
2630 Glendale Milford
Cincinnati, OH 45241
001 ATTN: Mr. Jerry Middendorf

McDonnell Douglas
P.O. Box 423
St. Charles, MO 63301
001 ATTN: Mr. Gerald Rogers

Sandia Laboratories
P.O. Box 969
Livermore, CA 94550
001 ATTN: Tech Library (RPT)

Conic Corp.
9020 Balboa Avenue
San Diego, CA 92123
001 ATTN: Mr. Martin Gold

MANDATORY CONTRACT DISTRIBUTION LIST (Continued)

Magnavox Co.
2829 Maricopa Street
Torrence, CA 90503
001 ATTN: Mr. J. Moses

TRW Systems
One Space Park
Redondo Beach, CA 90278
001 ATTN: Mr. R. Sansom

Frequency Electronics, Inc.
3 Delaware Drive
New Hyde Park, NY 11040
001 ATTN: Mr. Martin Bloch

IBM
Bldg 905A, Dept. M94
Owego, NY 13827
001 ATTN: Mr. G. Ver Wys

Harris Electronics
Systems Division
Mail Stop I-1470
P.O. Box 37
Melbourne, FL 32901
001 ATTN: Mr. W. McGann

McDonnel Douglass
Astronautics Co.
5301 Boise Ave.
Huntington Beach, CA 92647
001 ATTN: A3-135 Library Services

Hughes Aircraft Co.
Missile Systems Division
Mail Station B-90
Canoga Park, CA 91304
001 ATTN: Mr. C. French

MANDATORY CONTRACT DISTRIBUTION LIST (Continued)

SAMSO-YEE
Headquarters
Space & Missile System
Organization
P.O. Box 92960
Worldway Postal Center
Los Angeles, CA 90005

001 ATTN: Lt. Col. Goldtrap
001 ATTN: Mr. John Dewall
001 ATTN: Col. Henderson
001 ATTN: Lt. Karl Kovach

Northern Illinois Univ.
I & T Dept
Dekalb, Ill 60115

001 ATTN: D. E. Newell

RADC/ETS
Hanscom AFB, Mass 01731

001 ATTN: A. Kahan

JHU/Applied Physics Lab
John Hopkins Road
Laurel, MD 20810

001 ATTN: J. R. Norton

ITT Aerospace/Optical Div
3700 East Pontiac
Ft. Wayne, Indiana 46803

001 ATTN: Mr. James Chen

Hughes Aircraft Company
500 Superior Ave.
Newport Beach, CA 92663

001 ATTN: H. E. Dillon

Rockwell International
Government Avionics Division
400 Collins Avenue
Cedar Rapids, Iowa 52406

001 ATTN: Mr. Bill Howard

MANDATORY CONTRACT DISTRIBUTION LIST (Continued)

Magnavox Advanced Products Division
2829 Maricopa Street
Torrence, CA 90503
001 ATTN: Mr. David L. Hessick

Boeing Aerospace Corp.
P.O. Box 3999, Mail Stop 8805
Seattle, Washington 98124
001 ATTN: Mr. Jim W. Bieber

Stanford Telecommunications Inc.
1195 Bordeau Drive
Sunnyvale, CA 94086
001 ATTN: Mr. Julius Ville

Savoy Electronics
P.O. Box 5727
Ft. Lauderdale, FL 33310
001 ATTN: Mr. Eugene Lussier

HDQ, TCATA
Fort Hood, TX 76544
001 ATTN: ATCAT-IA-I (Mr. J. Austin)

ASD/XRQ-NIS
Wright Patterson AFB, Ohio 45433
001 ATTN: Cpt. Michael Gaydeski

RADC/ESE
Hanscom AFB
Bedford, MA 01731
001 ATTN: Dr. Nicholas Yannoni

Naval Research Lab
4355 Overlook Avenue
Washington, DC 20375
001 ATTN: Mr. David Philips, Coide 7524

General Electric Neutron Devices
P.O. Box 11508
St. Petersburg, FL 33733
001 ATTN: Mr. Robert Ney

MANDATORY CONTRACT DISTRIBUTION LIST (Continued)

Mitre Corp.
P.O. Box 208
Bedford, MA. 01730
001 ATTN: Mr. Gene O'Sullivan-MS E035
001 ATTN: Mr. Donald Newman-MSG100

MIT, Lincoln Lab
P.O. Box 73
Lexington, MA 02173
001 ATTN: Mr. Richard Bush

F&T Standards Section, 227-04
NBS
325 Broadway
Boulder, CO 80302
001 ATTN: Dr. Samuel R. Stein

Rockwell International
Collins Tele, Prod. Div.
855 35th Stree, N.E.
Cedar Rapids, IA 52406
001 ATTN: Mr. Marvin Frerking

Raytheon Company
Technology Development Laboratory
528 Boston Post Road
Sudbury, MA 01776
001 ATTN: Mr. DAve Robillard

Hewlett Packard
5301 Stevens Creek Blvd
Santa Clara, CA 95050
001 ATTN: Mr. John A. Kusters

705 Advisory Group on Electron Devices
201 Varick Street, 9th Floor
002 New York City, NY 10014

Isotemp Research, Inc.
Charlottesville, VA 22901
001 ATTN: Mr. Waltere D. Galla

MANDATORY CONTRACT DISTRIBUTION LIST (Continued)

Greenray
840 West Church Road
Mechanicsburg, PA 17055
001 ATTN: Mr. G. Kurzenknabe

Sentry Manufacturing Co.
Crystal Park
Chickasha, OK 73018
001 ATTN: Mr. Don R. Abel

Austron, Inc.
1915 Kramer Lane
Austin TX 78758
001 ATTN: Mr. George Price

McCoy Electronics Co.
Chestnut & Watts
Mt. Holly Springs, PA 17065
001 ATTN: Mr. J. Koproski

Q-Tech Corp.
11529 W. Pico Blvd
Los Angeles, CA 90064
001 ATTN: Mr. Howard Phillips

Spectrum Technology, Inc.
001 Goleta, CA 93101
ATTN: Mr. Harry Gruen

Bulova Watch Co.
61-20 Woodside Avenue
Woodside, NY 11377
001 ATTN: Mr. Phil Duckett

CTS KNIGHTS, Inc.
Sandwich, IL 60548
001 ATTN: Mr. Howard Hinnah

NASA Goddard Space Flight Center
Greenbelt, MD 20771
001 ATTN: Mr. Bernard Trudell, Code 480

MANDATORY CONTRACT DISTRIBUTION LIST (Continued)

Westinghouse Electric Corp.
P.O. Box 746
Baltimore, MD 21203
001 ATTN: Mr. Dan Healy, III, MS 378

Harris Corp.
Government Systems Group Operation
P.O. Box 37,
Melbourne, FL 32901
001 ATTN: Mr. David Leigh

Frequency & Time Systems
182 Conant Street
Danvers, MA 01923
001 ATTN: Dr. Hellmut Hellwig

Tracor, Inc.
6500 Tracor Lane
Austin, TX 78721
001 ATTN: Mr. Robert Hanks

MIT, Lincoln Lab
244 Wood Street
Lexington, MA 02173
001 ATTN: L. Laughlin (Library)